THE ROLE OF MARINE NUTRIENTS IN 2,3,7,8-TETRACHLORODIBENZO-*P*-DIOXIN TOXICITY *IN VITRO* AND *IN VIVO*

by

Eline Taksdal

This thesis is submitted in partial fulfilment of the requirements of the degree of Master of Science

Department of Biological Science

Faculty of Mathematics and Natural Sciences

University of Bergen

June 2022

THE ROLE OF MARINE NUTRIENTS IN 2,3,7,8-TETRACHLORODIBENZO-*P*-DIOXIN TOXICITY *IN VITRO* AND *IN VIVO*

by

Eline Taksdal

Master thesis in Molecular Biology

Institute Of Marine Research

Department of Seafood and Nutrition

Bergen

June 2022

ACKNOWLEDGEMENTS

The work presented in this thesis was performed at the Institute of Marine Research, department of Seafood and Nutrition in Bergen from August 2021 to June 2022.

First and foremost, I would like to express my greatest gratitude to my supervisor throughout this thesis, Ole Jakob Nøstbakken. He has provided me with invaluable mentorship and experiences in not just research, but also in the personal related aspects of science. I would especially highlight Nøstbakken's commitment and support through the many challenges and changes that arose throughout this thesis and for entrusting me with his resources. My time under Nøstbakken's mentorship has been highly educational and his knowledge within the field of molecular biology has been greatly inspiring.

Furthermore, I would like to express my gratitude to Kai Kristoffer Lie for letting me tag along during laboratory training and for helping me interpreting my controversial qPCR results. A special thanks to Hui-Shan Tung and Amalie von Barner Tvedegaard Heim for teaching me new methods in the molecular laboratory and for always offering their assistance and help. I would also like to thank the remaining members of the Seafood and Nutrition department, for always greeting me with a smile and making me feel welcome.

Thank you to all my fellow master students at "loftet" for the best company and amusing lunch breaks. Finally, I cannot thank my friends, family, and boyfriend enough for their invaluable support, for showing interest in my work, and for at least trying their best to wrap their heads around my field of interest.

Bergen, June 2022
Eline Taksdal

ABBREVIATIONS

AhR	Aryl hydrocarbon receptor
AhRR	Aryl hydrocarbon receptor repressor
ANOVA	Analysis of Variance
ARNT	Aryl hydrocarbon receptor nuclear translocator
AUC	Area under curve
BSA	Bovine serum albumin
cDNA	Complementary DNA
CONTAM	Contaminants in the food chain, EFSA expert panel
Cyp	Cytochrome P450
DHA	Docosahexaenoic acid
dl-PCB	Dioxin-like polychlorinated biphenyl
DMEM	Dulbeccos modified eagle's medium
EFSA	European food safety association
EPA	Eicosapentaenoic acid
FA	n-3 fatty acids
FBS	Fetal bovine serum
HSP90	Heat shock protein 90
NOAEL	No observed adverse effect level
PBS	Phosphate buffered saline
PCB	Polychlorinated biphenyl
PCDD	Polychlorinated dibenzo-*p*-dioxin
PCDF	Polychlorinated dibenzofuran
PUFA	Polyunsaturated fatty acid
qPCR	Real time quantitative polymerase chain reaction
REP	Relative effect potency
RPMI	Roswell Park Memorial Institute
RTCA	Real time cell analyser
SD	Standard deviation
SDS-PAGE	Sodium dodecylsulphate-polyacrylamide gel electrophoresis
TCDD	2,3,7,8-Tetrachlorodibenzo-*p*-dioxin
TEF	Toxicological equivalent factor
TEQ	Toxic equivalent quotient
TWI	Tolerable weekly intake
VKM	Vitenskapskomiteen for mat og miljø
WHO	World health organization

ABSTRACT

2,3,7,8-Tetrachlorodibenzo-*p*-dioxin (TCDD) is the most potent dioxin congener and is associated with several adverse health effects. As a result of its high lipophilicity and slow degradation the compound easily accumulates in the environment and foods. A prominent source for human exposure to TCDD is through the consumption of fatty fish. However, fatty fish is also a prominent dietary source for the essential 3-n fatty acids DHA and EPA. Risk-benefit analyses consistently concludes that the health benefits obtained through fish consumption outweighs the risk of dioxin exposure. However, in 2018 EFSA reduced the tolerable weekly intake (TWI) by 7-fold for dioxin and dl-PCBs in foods. The reduction was based on a longitudinal study investigating the negative effects in semen parameters by dioxin and dl-PCBs in Russian boys.

The aim of the present study was to investigate if TCDD can induce a similar toxic response in testis as in the liver, and if the toxicity is related to the induction of the aryl hydrocarbon receptor. Furthermore, potential interactions between TCDD and n-3 fatty acids was investigated, to examine whether n-3 fatty acids can affect TCDD toxicity. The aims were investigated using *in vitro* and *in vivo* models. Established cell lines, including hepatocytes, Sertoli, and Leydig cells, were pre-incubated with n-3 fatty acids prior to TCDD exposure. Additionally, a previously performed animal study based on salmon fed mice was included to examine the potential differences in established cell lines and in a complete biological system.

The aims were primarily investigated using cell impedance assay, and protein- and gene expression analysis. The present study demonstrates lack of Cyp1a1 expression in testis at protein- and gene level and highlights possible alternative TCDD-mediated responses. Analyses of hepatocytes and Sertoli cells identified no significant interaction effects between TCDD and n-3 fatty acids. Nor a significant interaction between TCDD and marine nutrients was observed. A distinct difference in Cyp1a1 protein expression in liver was observed *in vitro* versus *in vivo*. Cyp1a1 was only observed in *in vitro* hepatocytes.

The results of the present study indicate that alternative mechanisms are involved as TCDD-mediates its toxicity in testis. Interaction effects between TCDD and n-3 fatty acids was not observed in this study. However, n-3 fatty acids' potential in protecting against the effect of TCDD toxicity is promising and should thus be further elucidated.

TABLE OF CONTENTS

1. INTRODUCTION

1.1 DIOXINS AND POLYCHLORINATED BIPHENYLS

Dioxin is a collective term for chlorine-containing groups and is further divided into polychlorinated dibenzo-*p*-dioxins (PCDD) and polychlorinated dibenzofuran (PCDF). PCDDs/Fs consist of tricyclic planar compounds (figure 1) constituting 75 and 135 congeners, respectively, depending on the number and positioning of chlorine atoms at the carbon rings (EFSA CONTAM, 2018). Dioxins are unintentionally produced by-products formed during burning or combustion processes, as well as some industrial processes. I.e., the production of metals and more natural sources such as forest fires, to mention some. The general prerequisite is high-temperature processes in the presses of chlorine and carbon (Kanan & Samara, 2018).

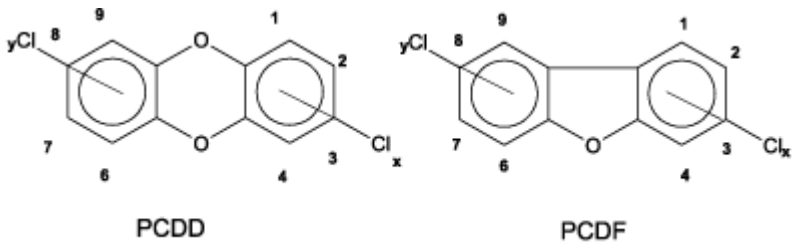

Figure 1: General structure of PCDD and PCDF. Cly and Clx indicate the possible composition, by the carbon positions, of chlorine atoms on the compound constituting the variety of congeners. Retrieved from Pereira (2004).

Polychlorinated biphenyls (PCB) consist of two compound benzene rings linked together at the C1 carbon (figure 2). With a variety of 1-10 chlorine atoms in an *ortho, meta,* and/or *para* position, 209 congeners are possible compounds of PCB. In contrast to dioxins, PCB is a man-made product and was produced from the late 1920s until banned around the 1980s (Mozaffarian & Rimm, 2006). Usually, the commercial-made PCBs were complex mixtures constituting 60-90 congeners (Wiegel & Wu, 2000) and were frequently applied due to their chemical and physical properties as flame resistance, their stability to oxidation, and low water solubility, to mention some (Kimbrough & Jensen, 2012). A dozen of the 209 PCB congeners show similar biological and chemical activity as PCDD/F. Hence, these twelve PCBs exhibit dioxin-like properties and are therefore named dioxin-like PCBs (dl-PCB) (Erickson & Kaley, 2011).

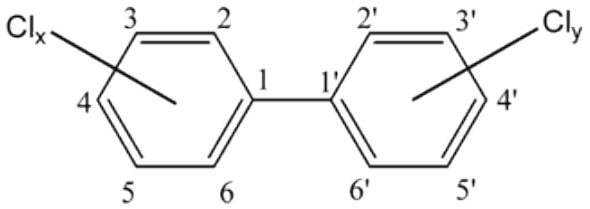

Figure *2*: General structure of PCB. Cly and Clx indicate the possible composition, by the carbon positions, of chlorine atoms on the compound constituting the variety of congeners. Adapted from Erickson (2018).

1.2 Toxicity of Dioxins and Polychlorinated Biphenyls

Of the many PCDD/F congeners only seven and ten, respectively, exhibit dioxin-like toxicity. These dioxin congeners have a chlorine substitution in the lateral 2, 3, 7, and 8 positions (and will be referred hereafter as "dioxins"), and the dl-PCBs have chlorine atoms located in a meta- and/or para position (Justino et al., 2016; Kulkarni, Crespo, & Afonso, 2008). Some common features of dioxins and dl-PCBs are their high affinity and toxic- and biological activity for the cytosolic aryl hydrocarbon receptor protein (AhR) – one of several protein "sensors" participating in detecting cellular milieu changes (Erickson & Kaley, 2011; Van den Berg, De Jongh, Poiger, & Olson, 1994). Furthermore, dioxins and dl-PCBs are designated as persistent organic pollutants (POP). They have been titled as such due to their slow degradation in the environment and as they are excreted to a small extent from exposed organisms. Hence, leading to bioaccumulation of the toxicant in various animal species (Bolann et al., 2017).

Among the dioxins and dl-PCBs, 2,3,7,8-Tetrachlorodibenzo-*p*-dioxin (TCDD) is the most potent in causing toxicity and is, therefore, the prototype to which toxicological actions of the remaining dioxin-like congeners are compared. This comparison is often referred to as the toxicological equivalent factor (TEF) and provides a toxicity indication of the congener in question relative to TCDD (Van den Berg et al., 2006). A congener's TEF value is further derived from several relative effect potency (REP) measurements, which is determined by the congener's individual possibility for producing toxic or biological effects relative to a reference compound, usually TCDD. REP values are usually determined by various *in vivo* and *in vitro* studies, and it is by the World Health Organisation's (WHO) expert panel that these results are evaluated to agree on appropriate TEF values on an international level (Haws et al., 2006; Van den Berg et al., 2006). From the TEF approach, additive effects can be calculated by summing the products of a single congener's concentration or dose multiplied by its corresponding TEF, resulting in toxic equivalent quotients (TEQ) of existing mixtures (Van den Berg et al., 2006).

Table 1: A selection of dioxin and dl-PCB congeners.

Abbreviation	Compound	TEF	Illustration
TCDD	2,3,7,8-Tetrachlorodibenzo-*p*-dioxin	1	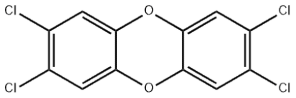
HxCDF	1,2,3,4,7,8-Hexachlorodibenzofuran	0.1	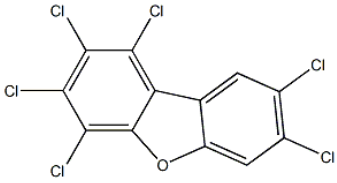
PCB 126	3,3´,4,4´,5-Pentachlorobiphenyl	0.1	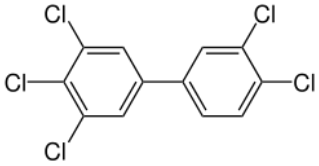

PCDD, PCDF, and dl-PCB are each illustrated by one of their congeners: TCDD, HxCDF, and PCB126, respectively, with corresponding TEF values. The corresponding TEF-values are retrieved from the WHO's re-evaluation of TEF values from 2005. Adapted from Van den Berg et al., 2006.

1.2.1 TOXICOKINETIC AND TOXICODYNAMIC

Dioxins and dl-PCBs can be found in various sources in the environment (Fernandez-Gonzalez, Yebra-Pimentel, Martinez-Carballo, & Simal-Gandara, 2015). Due to the chemical's lateral chlorine atoms, and therefore their highly lipophilic properties, they tend to switch from a hydrophilic- to a hydrophobic environment. Usually, i.e., living organisms with lipid cell structures (EFSA CONTAM, 2018). The toxicant can enter an organism through various absorption routes, however, most commonly through the gastrointestinal tract. Hence, as dioxins and dl-PCBs easily bioaccumulate, indicates food to be the most prominent source for exposure. Once absorbed into the body the toxicants are extensively distributed throughout the body via the cardiovascular system (Suzuki, Nakano, & Nakano, 2005) and subsequently mainly retained in fat and liver tissue (Van den Berg et al., 1994). As the number of chlorine atoms increases on a congener, so does its chemical stability and lipophilicity. Hence, dioxins and dl-PCBs are relatively resistant to hydrolysis and subsequently metabolism. This provides dioxins and dl-PCBs with an extensive half-life, which varies greatly between species (Aune, 2007). Though challenging, the possibility for metabolism and elimination of these substances is through transformation into polar metabolites. Such biotransformation involves an epoxidation of the molecules with the formation of hydroxyl-derivates (phase I) and

conjugation by phenol, glucuronidation, etc. (phase II). Through phase I, cytochrome P-450 (Cyp) isozymes, e.g., CYP1A1, are activated causing a cascade and subsequently an oxidated intermediate product that is more polar and less toxic than its parental molecule. Hence, the metabolism of dioxins and dl-PCBs can be viewed as a decontamination pathway (Aune, 2007; Pereira, 2004). The metabolism of dioxins and dl-PCBs act as a rate-limiting step for elimination, highlighting the substance's potential for bioaccumulation in suitable tissues. If unmetabolized, dioxins are partially eliminated through excrements. When metabolized, however, the metabolite can be eliminated partially through the gall, excrements, and to a small extent through urine, increasing elimination routes (Pereira, 2004).

Though AhR is a highly conserved protein across species the lethal dose for TCDD necessary to euthanize 50% (LD_{50}) of distinct species show great variation (Table 2). This may be a result of differences in terms of toxicity handling proteins and their conservancy between species (Aune, 2007).

Table 2: Lethal dose of TCDD in different animals.

Specie	LD_{50} (µg/kg BW)
Rat	2
Rhesus monkey	~70
Mouse	100-300
Hamster	~3000

The LD_{50} indicates the required dosage of TCDD to reduce the population by half. Adapted from Pohjanvirta and Tuomisto (1994).

AhR is a member of the basic Helix-Loop-Helix PER-ARNT-SIM (bHLH-PAS) family of transcription factors that regulate a variety of physiological and developmental processes (Kanan & Samara, 2018). AhR exists as a cytosolic complex with chaperones including two molecules of heat shock protein 90 (Hsp90), and one molecule each of immunophilin-like protein hepatitis B virus X-associated protein 2 (XAP2) and prostaglandin E synthase 3 (p23), when in its non-ligand bound state (Petrulis & Perdew, 2002). Once dioxin and dl-PCB are absorbed in the body, e.g., TCDD diffuses through the cell membrane and binds to AhR. As TCDD attaches to the cytosolic complex one Hsp90 as well as both p23 and XAP2 are

disassociated. Subsequently, translocating the formed AhR-TCDD complex into the nucleus. Inside the nucleus the AhR-TCDD complex heterodimerizes with the AhR nuclear translocator (Arnt) at their respective PAS domains, leading to the release of the second Hsp90. Further, as the AhR-TCDD-Arnt complex is formed, binding to DNA at dioxin response elements (DRE) in the promoter region of target genes may then occur and transcription may proceed. By hijacking AhR, thus disrupting its endogenous function, dioxins and dl-PCBs are believed to maintain a persistent activation of AhR. Consequently, preventing the AhR from functioning in homeostasis maintenance and thus induce dioxin and dl-PCB toxicity (Marlowe & Puga, 2005; Singh, Casado, Opanashuk, & Gasiewicz, 2009).

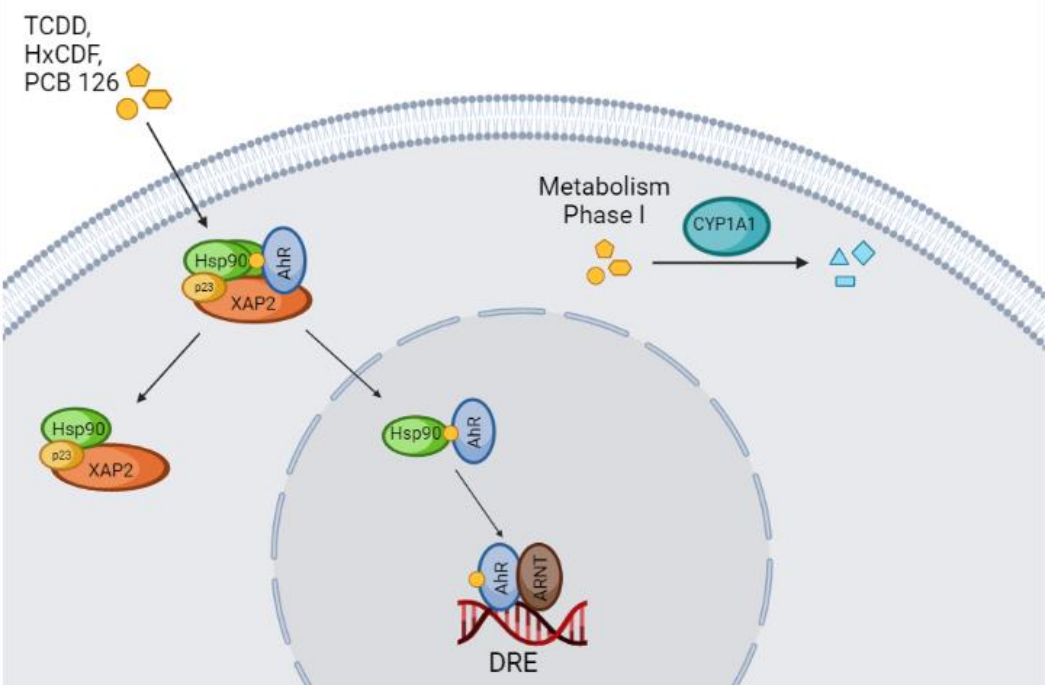

Figure 3: AhR signalling pathway. The canonical AhR pathway is initiated by diffusion of dioxins or dl-PCBs following binding to the cytosolic AhR complex, leading to a dissociation of the components bound to the AhR complex, all but one Hsp90 compound. The newly formed complex translocates into the nucleus and subsequently heterodimerize with ARNT, leading to the dislocation of Hsp90. Further the AhR-dioxin-ARNT complex may bind to dioxin response elements (DRE) in DNA, upregulating transcription of target genes. Modified from Matthews J. AHR toxicity and signaling: Role of TIPARP and ADP-ribosylation. Current Opinion in Toxicology. 2017;2:50-57. Created in BioRender.

Though the aforementioned canonical pathway for AhR-mediated toxicity is considered as the most common in dioxin and dl-PCB toxicity (EFSA CONTAM, 2018), the structural diversity of AhR's ligands may cause it to interact with various receptor-mediated signalling pathways and could explain its pleiotropic effects. AhR activation may thus be engaged in cell cycle regulation, mitogen-activated protein kinase cascades, immediate-early gene induction, and

crosstalk with other signalling molecules (El-Sabeawy et al., 1998; Henley, Bellone, Williams, & Ruh, 2004; Long, Pray-Grant, Tsai, & Perdew, 1998; Sorg, 2014; Tian, Rabson, & Gallo, 2002; Williams, Son, & Terranova, 2004). At final steps the AhR undergoes proteasomal degradation (Coelho et al., 2021)

1.3 Directive of Dioxins and Polychlorinated Biphenyls

As a result of the persistency and hazardous effects of dioxins and dl-PCBs these compounds have been subject to regulation and the establishment of guidelines. Regulation through public authority and industry efforts have reduced emissions by 90% from 1977 to 2006 (Mozaffarian & Rimm, 2006), hence steadily reducing their presence in food and feed. Nevertheless, due to the characteristic properties of dioxins and dl-PCBs their abundance in the environment is altogether sustained (Jensen, Eilertsen, Otnæs, Mæhre, & Elvevoll, 2020). In 2001 the European Union adapted a strategy to further reduce contamination levels of dioxins and dl-PCBs in the environment and feed and foods to ensure a high level of protection of the public health. As part of achieving this goal maximum levels (ML) for dioxins, and which was further extended with dl-PCBs in 2006 (European Food Safety Authority, 2012), were established. The ML parameter states food not complying with the MLs are not to be used as, or mixed with, food ingredients or other foods. MLs are in general around the 90^{th} percentile of the respective frequency distribution and expressed as pg TEQ/g using the WHO_{2005}-TEFs (EFSA CONTAM, 2018). Though various tools have been implemented, the public is nonetheless exposed to dioxin and dl-PCB through consumption. Thus, a tolerable limit has been established and is based on the concentration of dioxins and dl-PCBs consumable throughout life without increased health risk, commonly described as the no observed adverse effect level (NOAEL). For dioxins and dl-PCBs EFSA has implemented the limit as tolerable weekly intake (TWI), meaning the limit is set based on tolerable exposure per week. In 2018 EFSA published a new risk assessment (EFSA CONTAM, 2018) for animal and human health related to the presence of dioxins and dl-PCBs in feed and food. The assessment published a re-evaluation of the TWI set in 2001 and reduced it by seven-fold to 2 pg TEQ/kg bw per week (EFSA CONTAM, 2018). The TWI re-evaluation was based on the relationship between reduced sperm concentrations and serum dioxin-TEQ levels from a study examining environmental exposure in children over a decade (Mocarelli et al., 2008). Interestingly, the study included a narrow age distribution and may thus be elusive as the TWI regulation apply to all consumer categories (Unit on Biological Hazards and Contaminants, 2018). The Joint FAO/WHO Expert Committee on Food Additives

(JECFA), however, derived in 2001 a tolerable monthly intake (TMI) of 70 pg TEQ/kg bw in which still stands unchanged. JECFA's TMI is derived from two studies that consists of one linear model and one power model in order to extrapolate maternal body burden, where the Committee decided on a mid-point of the results' range (JECFA, 2002).

Various events throughout time such as the industrial accident in Lundwigshafen in 1953 (Thiess, Frentzel-Beyme, & Link, 1982) and in Seveso in 1976 (Assennato, Cervino, Emmett, Longo, & Merlo, 1989), have contributed to increased dioxin and dl-PCB levels in the environment. Production of chlorine-containing chemicals have also contributed to these elevated levels and subsequently increased background exposure to the proximate population (Mínguez-Alarcón et al., 2017). Though unfortunate it provides first-hand material to further understand the effects of acute and sustained human exposure to these toxicants. Following the Seveso accident, retrospective studies found a reduced male/female ratio in infants born to males post TCDD exposure (Mocarelli et al., 2000), as well as an endocrine disruptive activity affecting semen quality in young males (Mocarelli et al., 2008). Another study utilizing human extrapolated samples is the Russian Children's study (Mínguez-Alarcón et al., 2017). The study is a cohort study spanning over a decade emphasizing the influence of childhood environmental exposure in regard to the reproductive health of Russian males exposed to dioxin and dl-PCB. In summary, Mínguez-Alarcón and colleagues found that lower semen parameters were associated with greater peripubertal serum TCDD concentrations and PCDD TEQs (Mínguez-Alarcón et al., 2017). Though debated in hindsight, the EFSA Panel estimated a new value for the no-observed-adverse-effect level (NOAEL) and proposed a new value for the total TWI based on the results of the Russian Children's study. The problem, however, concerns the study's narrow age distribution, pre-puberty and puberty, as the rules in force regarding TWI apply to all consumer categories (Unit on Biological Hazards and Contaminants, 2018).

1.4 MARINE N-3 FATTY ACIDS

N-3 fatty acids (FA) consist of long chain polyunsaturated fatty acids, with its first carbon-carbon double bond located at C3 counting from the methyl end. FAs can be divided into two subgroups. One derived from seafood, which includes i.a., docosahexaenoic acid (DHA, 22:5n-3) and eicosapentaenoic acid (EPA, 20:5n-3). The other group includes the plant oil-derived α-linolenic acid (ALA, 18:3n-3) (Spector, 1999). The latter can to some extent be elongated and desaturated to DHA and EPA in humans. However, the self-synthesized levels are not adequate

for optimal function, and humans are thus dependent on acquiring these nutrients. DHA and EPA are designated as marine FAs considering their abundance in fish and seafoods. The FA content can vary greatly between fish species, being high in fatty fish like salmon and relatively low in lean fish like cod (Schmidt, Arnesen, de Caterina, Rasmussen, & Kristensen, 2005). The marine FA's role in human physiology is pivotal due to their incorporation and viscosity attribution to various cell membranes, and to their role in anti-inflammatory processes. DHA is mostly incorporated in neurological cell membranes, whereas EPA has been mostly observed as an important therapeutic within mental health (Swanson, Block, & Mousa, 2012).

DHA and EPA are metabolized by three main oxidative pathways, which include lipoxygenase (LOX), cyclooxygenase (COX) and Cyp. Through these pathways, different oxidized lipid mediators, designated oxylipins, are produced (Bazinet & Layé, 2014). Oxylipin formation is triggered by cell activation, leading to release of FAs from the sn-2 position via cytosolic phospholipase A2 (cPLA2). The most commonly studied oxylipins include eicosanoids and docosanoids from EPA and DHA, respectively (Chavan-Gautam, Rani, & Freeman, 2018).

1.5 Risk-Benefit Associated with Fish in the Diet

Though seafood is an important source of DHA and EPA, it is also the most prominent source for dioxins and dl-PCBs to humans. The POP's bioaccumulation in the environment and animals subsequently make foods the main source of human exposure to dioxins and dl-PCBs (EFSA CONTAM, 2018). Henceforth, risk-benefit analyses have been conducted assessing the risk related to dietary exposure through sources of essential nutrients (EFSA CONTAM, 2018; VKM, 2022). In May 2022 the Norwegian Scientific Committee for Food and Environment (VKM) published an assessment of dioxins and dl-PCBs in food in Norway (VKM, 2022). The assessment concluded that the mean dioxin and dl-PCB exposure of the Norwegian population is above the TWI. However, previous comprehensive risk-benefit assessments conducted by both EFSA and VKM, concluded that the dioxin and dl-PCB exposure from fish represents a negligible risk and is of no concern, as the health benefits from consuming fatty fish outweigh the hazardous risk related to exposure (EFSA CONTAM, 2018) (VKM, 2014). A re-assessment of VKM's 2014 risk-benefit assessment is scheduled in June 2022.

The adverse effects of TCDD toxicity have shown to cause reproductive and developmental problems, damage the immune system, interfere with hormones, cause cancer, and induce

oxidative stress (Furue, Ishii, Tsukimori, & Tsuji, 2021). Conversely, DHA and EPA may also affect the same systems as TCDD, however with positive effect on (Guo, Tong, Ruan, Sinclair, & Li, 2020). However, little is known about the possible interaction of these compounds. Though few studies are available, it is suggested that marine FAs may play a pivotal role in protecting against TCDD toxicity (Wiest, Walsh-Wilcox, Rothe, Schunck, & Walker, 2016).

1.7 *IN VITRO* VERSUS *IN VIVO* MODELS

In vitro models are used when examining biological mechanisms in a controlled environment outside of its natural system. The simulated environment is supposed to replicate the natural conditions in order to best examine the mechanisms in question. By isolating a single cell line from a living organism however, possible cellular and endocrine interaction effects are ignored. Therefore, *in vivo* models may be used to obtain a more comprehensive result. The use of *in vivo* models includes whole living organisms and may thus produce a precise picture of biological mechanisms. An *in vivo* experiment may however be complex and time-consuming (Dahman, 2019).

1.8 AIMS OF THE STUDY

N-3 fatty acids is well known for health beneficial effects, such as effects on the cardiovascular system and mental health. These nutrients may be found in several foods, though fatty fish is the most well-known source. Although fatty fish can provide the beneficial n-3 fatty acids, it may also contain environmental pollutants such as dioxin and dl-PCB. Dioxin and dl-PCB have shown to cause reproductive toxicity by affecting spermatogenesis and sperm quality. In EFSA's re-assessment of TWI the effects by dioxin and dl-PCB on male reproduction were pivotal.

Risk-benefit analyses of dioxin-contaminated foods consistently conclude that the nutritional benefits of n-3 fatty acids outweigh the cost of dioxin exposure (EFSA CONTAM, 2018; VKM, 2014). The interest of the present study was to improve our understanding of dioxin's toxicity when combined with marine nutrients and its effect on spermatogenesis. Therefore, the interest of the study was to explore the following:

i. does TCDD induce a similar toxic response in testis as in liver.

ii. is the potential TCDD toxicity in testis related to AhR induction.

iii. does n-3 fatty acids affect TCDD toxicity

2. MATERIALS

2.1 CHEMICALS AND REAGENTS

Table 3: Chemicals and reagents utilized throughout the fulfilment of the master thesis.

Name	Supplier	Catalogue number
100x Protease/Phosphatase Inhibitor Cocktail	Cell Signalling Technology	5872
10x PBS tablet	Thermo Fisher Scientific	18912014
10x Trisglycine SDS Buffer	Bio-Rad	161-0732
2x Laemmli Sample Buffer	Bio-Rad	161-0737
β-mercaptoethanol	Sigma-Aldrich	M3148
Amersham ECL Prime Western Blotting Detection Reagents	Sigma-Aldrich	RPN 2232
Chloroform	Avantor/VWR	CAS 67-66-3
Anti-CYP1A1 antibody	Abcam	ab235185
Dimethyl Sulfoxide (DMSO)	Merck	PHR1309
DNase I	Thermo Fisher Scientific	18068015
Docosahexaenoic acid	Merck	D2534
Dulbecco's Modified Eagle's Medium – High Glucose	Merck	D5671
Dulbecco’s Modified Eagle’s Medium/Nutrient Mixture F-12 Ham	Merck	D6421
ECL™ Blocking Agent	Sigma-Aldrich	RPN 2125
Eicosapentaenoic acid	Merck	E2011
Ethanol (100%, 75%)	Antibac	200-578-6
Fetal Bovine Serum	Thermo Fisher Scientific	10270106
GelPilot 50 bp Ladder	Qiagen	239025
Geneticin™ Selective Antibiotic	Gibco™	10131-035
Horse Serum	Merck	H1270
Methanol	Honeywell	67-56-1
N-Acetyl-L-glutamine	Merck	2490-97-3
pEGFP-N1/roGFP plasmid	University of Oregon	
Penicillin-Streptomycin	Merck	P4083
Phosphate Buffered Saline Tablets	Thermo Fisher Scientific	18912014

Precision Plus Protein™ Western C™ Standard	Bio-Rad	161-0376
Precision Protein StrepTactin-HRP Conjugate	Bio-Rad	161-0381
QIAzol Lysis Reagent	Qiagen	79306
RIPA Buffer	Sigma-Aldrich	R0278
RPMI-1640 medium	American Tissue and Cell Collection	30-2001
Sodium Acetate	Thermo Fisher Scientific	AM9740
TE buffer	A8569	PanReac AppliChem
Trans-Blot Turbo 5x Transfer Buffer	Bio-Rad	10026938
Trypan Blue 0.4%	Bio-Rad	1450013
Trypsin-EDTA Solution 1x	Merck	59428C
Tween® 20	Sigma-Aldrich	P1379

2.2 BUFFERS

Buffer	Content
1x PBS (pH 7.45)	5 g PBS tablet 500 ml dH_2O
1x Running buffer	100 ml 10x Trisglycine SDS Buffer 900 ml dH_2O
1x Transfer buffer	200 ml 5x Transfer buffer 600 ml dH_2O 200 ml ethanol
5% blocking buffer	1 g ECL Blocking Agent 20 ml 0.05% PBS-Tween
RIPA-Protease Lysis Buffer	1 µl 100x Protease/Phosphatase Inhibitor Cocktail 1 ml RIPA Buffer

Sample buffer	950 µl Laemmli Sample Buffer 50 µl β-mercaptoethanol
Washing buffer (0.05% PBS-Tween)	100 ml 10x PBS 500 µl Tween-20 900 ml dH_2O

2.3 TOXICANT

Table 4: Toxicant applied to expose cell lines.

Abbreviation	Compound	TEF	MW (g/mol)	Concentration (mg/ml)	Catalogue number
TCDD	2,3,7,8-Tetrachlorodibenzo-*p*-dioxin	1	321.96	0.05	1746-01-6

TEF-value obtained from WHO's re-evaluation of TEF values from 2005 (Van den Berg et al., 2006).

2.4 COMMERCIAL KITS

Table 5: Commercial kits utilized throughout the fulfilment of the master thesis.

Kit	Use	Supplier	Catalogue number
EZ1 RNA Tissue Mini Kit	RNA extraction from tissue	Qiagen	959034
Pierce 660 nm Protein Assay Kit	Protein quantification	Thermo Fisher Scientific	22662
QIAGEN OneStep RT-PCR Kit	Qualification of qPCR primer	Qiagen	210212
RNA 6000 Nano LabChip Kit	RNA quality	Agilent	5067-1511
RNeasy® Plus Mini Kit	RNA extraction from cell lines	Qiagen	74136

2.5 EQUIPMENT AND INSTRUMENTS

Table 6: Equipment and instruments utilized throughout the fulfilment of the master thesis.

Name	Use	Supplier
CFX96 Touch Real-Time PCR Detection System	RT-qPCR	Bio-Rad
Counting chamber (0.01 mm)	Cell counting	Hurts Sienctific
Biomek 4000	Pipetting	Beckman Coulter
E-Plate 96-well	Cell adhesion and cytotoxicity	Agilent Technologies
Forma™ Steri-Cycle™ CO_2 Incubator	Cell cultivation	Thermo Scientific
Jenco™ Inverted Compound Microscope	Cell maintenance	Merck
Mini-PROTEAN Tetra Cell	Electrophoresis	Bio-Rad
Mini-PROTEAN TGX Stain-Free gel (4-15%)	SDS-PAGE	Bio-Rad
Mr. Frosty™ Freezing Container	Cell preservation	Thermo Fisher
Nanodrop™ 1000	RNA quality and quantity	Thermo Fisher
Nunc® CryoTubes®	Cell preservation	Merck
Nunc EasYFlask 72 cm^2	Cell cultivation	Thermo Fisher
Nunc™ 15 ml conical sterile polypropylene centrifuge tubes	Diverse usage	Thermo Fisher
Polytron® PT 2100	Tissue homogenisation	Kinematica
Precellys® 24 homogenizer	Tissue homogenisation	Bertin Instruments
Trans-Blot® Turbo™ Transfer System	Turbo-blotting	Bio-Rad
xCELLigence RTCA SP	Cell adhesion and cytotoxicity	

2.6 SOFTWARE

Table 7: Software utilized throughout the fulfilment of the master thesis.

Software	Use	Supplier
Agilent 2100 BioAnalyzer	RNA quality	Agilent Technologies
Biorender	Figures	Biorender
CFX Mastero	qPCR data analysis	Bio-Rad
Excel	Data treatment	Microsoft
GraphPad Prism 8	Figures and statistics	GraphPad Software Inc
Image Lab 6.0.1	Depicting gel and blot	Bio-Rad
RTCA Software 1.2.1	Real-Time Quantitative Cell Analysis	Agilent Technologies

2.7 CELL LINES AND CELL MAINTENANCE

Table 8: Cell lines utilized throughout the fulfilment of the master thesis.

Cell line	Cell type	Tissue	Use	Supplier	Catalogue number
HEPA 1-6	Hepatocyte	Liver	Tolerance of TCDD in combination with marine nutrients	American Tissue and Cell Collection	CRL-1830
MLTC-1	Leydig	Testicular			CRL-2065
TM4	Sertoli				CRL-1715

Table 9: Complete Growth medium for cultivation of the utilized cell types.

Complete Growth Medium MLTC-1		**Complete Growth Medium TM4**		**Complete Growth Medium HEPA 1-6**	
Component	Concentration	Component	Concentration	Component	Concentration
RPMI-1640 medium	1X	Dulbecco's Modified Eagle's Medium/Nutrient Mixture F-12 Ham	1X	Dulbecco's Modified Eagle's Medium – High Glucose	1X
With		**With**		**With**	
Sodium bicarbonate	1.5 g/l	Sodium bicarbonate	1.2 g/l	Sodium bicarbonate	n/a
Glucose	4.5 g/l	Glucose	3.15 g/l	Glucose	4.5 g/l
Sodium pyruvate	1 nM	Sodium pyruvate	0.055 g/l	Sodium pyruvate	n/a
HEPES	10 nM	HEPES	15 nM		
L-glutamine	2 nM				
Supplemented with		**Supplemented with**		**Supplemented with**	
Fetal bovine serum	10%	Fetal bovine serum	10 %	Fetal bovine serum	10%
Penicillin-Streptomycin	1%	Penicillin-Streptomycin	1%	Penicillin-Streptomycin	1%
		Horse serum	5%		

2.8 POLYMERASE CHAIN REACTION

2.8.1 ONE-STEP RT-PCR

Table 10: Reaction mix and reaction set-up for One-step qPCR.

Reaction Mix		Set-Up	Time	°C	
5x Qiagen OneStep RT-PCR Buffer*	5 µl	Reverse transcription	30 min	50	
5x Q-Solution®	5 µl	PCR-activation	15 min	95	
dNTP-mix	1 µl	Amplification			
Forward primer	0.5 µl	Denaturing	15 sec	94	x35
Reverse primer	0.5 µl	Annealing	15 sec	60	
RNase-inhibitor	0.25 µl	Extension	1 min	72	
Qiagen OneStep RT-PCR Enzyme Mix	1 µl	Final extension	10 min	72	
dH_2O	10.75 µl				
RNA template	1 µl				

*With 12.5 mM MgCl

2.8.2 CDNA SYNTHESIS

Table 11: Reaction mix and reaction set-up for cDNA synthesis.

Reaction Mix		Set-Up	Time	°C
10x TaqMan RT Buffer	5 µl	Incubation	10 min	25
$MgCl_2$ (25 nM)	11 µl	Reverse transcription	60 min	48
DeoxyNTPs Mixture (10 nM)	10 µl	Revers transcription inactivation	5 min	95
Random Hexamer primers	2.5 µl			
RNase inhibitor (20U/µl)	1 µl			
Multiscribe Reverse Transcriptase	1.67 µl			

2.8.3 qPCR

Table 12: Reaction mix and reaction set-up for qPCR.

Reaction Mix		**Set-Up**	**Time**	**°C**	
Syber Green PCR Master Mix (2x)	2.8 µl	Pre-incubation	30 min	50	
Forward Primer	0.1 µl	Amplification			
Reverse primer	0.1 µl	Denaturing	10 sec	94	
dH_2O	5 µl	Annealing	10 sec	60	x35
		Extension	10 sec	72	
		Melting curve	5 sec	95	
			1 min	65	
		Cooling	10 sec	40	

2.8.4 qPCR PRIMES

Table 13: Primes used for qPCR analysis

Gene	Primer direction	Nucleotide sequence (5`-3`)	Supplier
TBP	F	ACC CTT CAC CAA TGA CTC CTA TG	
	R	ATG ATG ACT GCA AGC AAA TCG C	
β-actin	F	ATG GGT CAG AAG GAC TCC TAC G	
	R	AGT GGT ACG ACG ACC AGA GG	
Calnexin	F	GCA GCG ACC TAT GAT TGA CAA CC	
	R	GCT CCA AAC CAA TAG CAC TGA AAG G	
eef1a1	F	ACG AGG CAA TGT TGC TGG TGA C	
	R	GTG TGA CAA TCC AGA ACA GGA GC	
AhR	F	CCA TGT ATC AGT GCC AGC	
	R	AGC TGT CGA AAG CCC TTA CC	
Cyp1a1	F	CAT CAC AGA CAG CCT CAT TGA GC	
(primer 1)	R	CTC CAC GAG ATA GCA GTT GTG AC	
Cyp1a1	F	CCT CTT TGG AGC TGG GTT TG	Thermo
(primer 2)	R	TGC TGT GGG GGA TGG TGA AG	Fisher
Cyp1a2	F	AAG ACA ATG GCG GTC TCA TC	
	R	GAC GGT CAG AAA GCC GTG GT	
Catalase	F	CGG CAC ATG AAT GGC TAT GGA TC	
	R	AAG CCT TCC TGC CTC TCC AAC A	
Gpx4	F	GCA GGA GCC AGG AAG TAA TC	
	R	GGC TGG ACT TTC ATC CAT TT	
Ybx3	F	CAA GCG GCT AAT GGT CCA AAC C	
	R	GTT CTC AGT TGG TGC TTC ACC TG	
Ccin	F	TCC AGG AGA ACC TGT GGCTGA A	
	R	TCA TAC CGC CAC GCT GTC TTC A	
Gapdhs	F	TAC TGT TGT CCA GCT ACG GC	
	R	GCT CTG GGA TGA CTT TGC CT	

3. METHODS

3.1 CELL CULTURE CULTIVATION

The HEPA 1-6 cell line is an isolated subclone originating from the BW 7756 hepatoma of C57L/J mice. A hepatic trait examination revealed several serum secreted proteins. However, the activities of several liver-specific enzymes appeared to be absent in the hepatoma cells. The identification of differentiated properties of cultured cells allows the hepatoma cell line to be used in a variety of studies, including tissue-specific gene products, and the modulation of gene expression of genes governing differentiated phenotypes (Darlington, Bernhard, Miller, & Ruddle, 1980).

MLTC-1 is one of several clonal Leydig cell lines established from the transplantable Leydig tumour, M548OP. Further, MLTC-1 show specific receptors for hCG and LH binding and has been characterised with regard to the gonadotropin-responsive adenylate cyclase system. In response to hCG binding MLTC-1 cells accumulate cAMP and produce progesterone. Hence, it is suggested that MLTC-1 cells have a gonadotropin-responsive adenylate cyclase system in which includes a specific hormone receptor, a regulatory component, and a catalytic subunit (Rebois, 1982).

TM4 is a cell line derived from testis of immature BALB/c mouse and is identified to be of Sertoli cell origin. The identification is based on TM4's characteristics as the cell respond to FSH, and not by LH, by increasing cAMP activity. Further, TM4 cells have specific receptors for FSH and have been documented to metabolize progesterone (Matfier, 1980).

The methods described for cell cultures were carried out for HEPA 1-6 cells, MLTC-1 cells and TM4 cells, only differing in applied complete growth medium.

3.1.1 THAWING CELL CULTURES

The cells were rapidly thawed and transferred to a 15 ml Nunc tube containing tempered complete growth medium (1:10). Subsequently, the cell-medium mixture was centrifuged at 130 x g for 5 minutes and the supernatant carefully discarded. The formed pellet was resuspended in 1 ml of tempered complete growth medium and transferred to a 75 cm^2 T75 Nunc cell cultivation flask to a final volume at 15 ml.

3.1.2 Cell Growth- and Maintenance Conditions

The cells were cultured in their respective complete growth medium (Table 9) in humidified conditions at 37 °C and 5% carbon dioxide in a Forma™ Steri-Cycle™ CO_2 Incubator. Cells were subcultured 1:2 or 1:3, depending on the cell cultures' confluence level. Prior to cell dispersion by trypsin, all cell cultures were sufficiently washed in 1x PBS to ensure an adequate removal of FBS. Hence, the protease inhibitor α1-antitrypsin was removed from the liver- and testis cell culture medium, and the cell could thereafter be separated by 1x Trypsin-EDTA solution using 3 ml and 5 ml, respectively. Subsequently, the cell's respective complete growth medium, containing FBS, was added to inhibit trypsinization before distributing the dispersed cell culture to the preferred quantity of cell cultivation flasks or -plates. The cells were then placed back in the incubator at the above conditions.

3.1.3 Preserving Cell Cultures

As the distinct cell types were to be utilized thorough out the completion of this thesis several cultures were frozen for preservation. The cells were dispersed as mentioned and subsequently centrifuged at 130 x g for 5 minutes followed by carefully discarding the supernatant. The formed pellet was resuspended in 1 ml freeze medium (95% complete growth medium, 5% DMSO (v/v)) and transferred to a 1.8 ml Nunc CryoTube. The tube was put in a Mr. Frosty™ Freezing Container and stored at -80 °C over night. The following day the ampoule was relocated to a container with liquid nitrogen for prolonged storage. Hence, providing a gradual freezing of the cell cultures from 37 °C, to -80 °C to the final -196 °C.

3.2 xCelligence – Real Time Cell Analysis

With high accuracy and sensitivity, the Agilent xCelligence Real-Time Cell Analysis (RTCA) continuously monitors cell behaviour through its impedance spectroscope. As a non-invasive and label-free assay, the impedance measurement produces real-time cell culture monitoring. A set of gold microelectrodes fused at the bottom surface of an electronic microtiter plate (E-plate) represents the functional unit of the cellular impedance assay. The application of an electric potential across these electrodes when submerged in an electrically conductive solution, such as buffer or standard cell medium, causes electrons to exit the negative terminal, pass though bulk solution, and deposit into the positive terminal completing the circuit. Consequently, as this phenomenon depends on the interaction of electrodes with bulk solution, the interference of adherent cells at the electrode-solution alters electron flow. Hence, the

impedance's magnitude reflects cell quantity and morphology (Agilent, 2022). The electron flow is reported by the unitless Cell Index (CI) parameter, where

$$CI = \frac{(Impendance\ at\ point\ n - Impendance\ in\ the\ absence\ of\ cells)}{Nominal\ impendance\ value}$$

3.2.1 Cell Proliferation and Cellular Confluence

The logarithmic growth phase of cells is the phase where cells actively proliferate and increase exponentially in cell density. At this state the population is considered to be the most viable (Ernst, Dombroski, & Merrick, 1990) and it was therefore considered necessary to determine the time of this state in regard to TCDD exposure. Hence, various cellular concentrations ranging from 5 000 – 100 000 cells per cm^2 were seeded in an E-plate and subsequently, by utilizing the xCelligence technology, the optimal starting concentration of cells per cm^2 was determined. After dispersing the cells by trypsin, the cells were manually counted using a counting chamber and trypan blue. The volume cell suspension required for the wanted cellular concentration was calculated and diluted in complete growth medium. After seeding cells in the E-plate the impedance background was measured. This measure was performed after adding of the cells in regard to possible ionic changes in the complete growth medium. Following, the cells were monitored by the RTCA system with one sweep every 30 minutes for 96 hours in humidified conditions at 37 °C and 5% carbon dioxide.

3.2.2 TCDD Dose-Response

To study the effect of TCDD exposure in combination with fatty acids (FA), an appropriate TCDD dose-response was established. The optimal TCDD-concentration would be a dose appropriate for affecting the cell culture but not stress the culture to initiate apoptosis. The dose-response relationship was determined by utilizing the xCelligence technology. HEPA 1-6, TM4 and MLTC-1 cells were seeded in an E-plate at 15 000 cells per cm^2, 16 700 cells per cm^2, and 15 000 cells per cm^2, respectively. After approximately 48 hours the cells were exposed to TCDD, ranging from 1 pM – 100 nM, or their medium changed. Subsequently, the cells response to TCDD exposure were monitored by the RTCA system with one sweep every 30 minutes for 72 hours post exposure.

3.3 Coupling of Fatty Acids to BSA

To ensure cell-uptake of DHA and EPA, the poorly water-soluble fatty acids were coupled to fatty acid free bovine serum albumin (BSA) – a suitable method for distributing FA to cells due to BSA's resemblance to the physiological system of nonesterified FA transport (Alsabeeh, Chausse, Kakimoto, Kowaltowski, & Shirihai, 2018). The FA-BSA coupling was carried out as described by Ghioni et al. (1997). 0.04 ml chloroform per mg FA was added. Further, the chloroform was evaporated under N_2, followed by addition of potassium hydroxide (KOH) at a 1:3 relationship and shaken in a whirl mixer for 10 minutes. BSA was then added to the FAs at a 2.5:1 relationship and shaken for 45 minutes. Following, the solution was sterile filtered (0.2 µm) and stored anoxic at -20 °C.

3.4 Interactions between TCDD and Marine Nutrients

Marine nutrients were introduced to cell cultures or mice for in *in vitro* and *in vivo* analysis, respectively.

3.4.1 *in vitro* Cell Study

HEPA 1-6 and TM4 cell cultures were pre-incubated in FA (60 µM), being DHA or EPA, or vehicle-BSA (60 µM) prior to TCDD exposure. Pre-incubated FA HEPA1-6 and TM4 cells were seeded according to the set seeding concentrations at 15 000 cells per cm^2 and 16 700 cells per cm^2, respectfully. Induced cell toxicity was assessed by cell growth impedance assay, western blot, and qPCR analysis

3.4.2 *in vivo* Animal Study

An animal study previously performed at the Institute of Marine Research, provided the *in vivo* samples used in this study. 80 male C57BL/6J mice modified with human AhR were divided into a total of 8 groups (n=10). Each group was chronic exposed to a distinct dioxin congener for 13 weeks and fed with casein (control diet) or salmon. In this study, only the group exposed to TCDD were employed for analysis. Furthermore, liver- and testicular tissue were extrapolated from the employed group and assessed by western blot and qPCR analysis.

3.5 Cell and Tissue Lysis

The analysis of intracellular components of cell cultures or tissues are initiated by separation into subcellular components. This is to enrich target protein and improve detection of low abundance proteins. This is carried out by homogenization where the plasma membrane is shredded, delimiting the cell, and thereby releasing its cellular contents. Homogenization can be carried out by numerous techniques e.g., by freezing and thawing or by high-speed blending. These techniques disrupt the cell membrane whilst leaving the majority of the cell relatively intact. The resulting homogenate can thus be separated into its component parts based on their density and size, which usually is done by centrifugation. The centrifugation speed and -time is determined by the subcellular component of interest, where the higher the speed and the longer the time centrifugated results in smaller components collected in a pellet (Feher, 2017).

3.5.1 Cell Lysis

Cells were seeded in a 6-well plate with complete growth medium and subsequently exposed to 10 nM and 100 nM TCDD. The cells were exposed when the culture had reached a confluence level of approximately 80%. 24 hours post exposure the cells were harvested by replacing complete growth medium with 200 µl RIPA-Protease Lysis Buffer and manually detached using a cell scraper. Due to the small sample volume, and to avoid protein dilution, the cells were lysed by repeated cycles of freezing and thawing. As ice crystals develop during the freezing process and subsequently contract after thawing, this method of lysis causes cells to expand and eventually rupture (Moutinho, Kingham, & D'Angelica, 2017). After homogenisation, the samples were centrifuged at 20 817 x g at 4 ℃ for 20 minutes. Leading to a fractionation of cell debris and cytosolic components in the visual form of a pellet and supernatant, respectively. Hence, the pellet was discarded, and the supernatant collected for further analysis.

3.5.2 Tissue Lysis

Liver- and testicular tissue originating from male C57BL/6J mice modified with human AhR from a previously carried out animal trail were implemented for *in vivo* comparison. Approximately 100 mg tissue were mixed with 200 µl RIPA-Protease Lysis Buffer and shredded by high-speed blending, using a Polytron PT 2100 for 3x30 seconds. The homogenised samples were centrifuged at 20 817 x g at 4 °C for 20 minutes. For, as aforementioned, lysis of cell debris and cytosolic components, following supernatant collection.

3.6 Protein Concentration Quantification

For further analysis the protein concentration of the fractionated samples was determined. Total protein concentration was quantified for all samples by Pierce 660nm Protein Assay. The assay is based on protein binding to a proprietary dye-metal complex in acidic conditions, leading to a shift in the dye's absorption maximum. The presence of positively charged amino acid groups facilitates a low pH and subsequently a colour change by deprotonation in the dye. Meaning the dye primarily interacts with the basic residues in proteins (Thermo Fisher Scienific, 2022).

150 µl Pierce 660nm Protein Assay Reagent was added to 10 µl supernatant from each sample, 10 µl Pre-Diluted Pierce Bovine Serum Albumin Standards, and 10 µl RIPA-Protease Lysis Buffer – serving as a blank for absorbance normalisation. All samples were mixed in a 96-well plate as triplicates. The plate was further covered and incubated while shaken for 1 minute, followed by 5 minutes of incubation at room temperature. Absorbance was measured at 660 nm by a VICTOR Multilabel Plate Reader, and generated the measurements required to make a standard curve form the BSA-standards. Subsequently, protein concentrations in all samples were calculated from the standard curve and normalised by subtracting the absorbance of the blank.

3.7 Western Blot

Western blot is a method for identifying proteins after separation by electrophoresis. A sodium dodecylsulphate-polyacrylamide gel electrophoresis (SDS-PAGE) separates proteins according to molecular weight. Separation is achieved by denaturing the proteins with a reducing agent and heat, and by adding SDS – a strong ionic detergent. SDS is a negatively charged complex and binds hydrophobically to proteins, thereby masking the protein's original charge. Furthermore, the protein is converted into a rod-shaped molecule with a mass-charge ratio dependent on the number of amino acids. A SDS gel consists of two parts – a stacking gel and a separating gel. The lower concentrated matrix gel of the stacking gel leads to a protein stacking at the border of the two gels, enabling a more precise separation. The gel is then transferred to a polyvinylidene difluoride (PVDF) membrane. A PVDF membrane has a high affinity for protein binding, primarily through dipole and hydrophobic interactions. The membrane's positively charged groups are activated by pre-treatment with methanol. Thereby facilitating the binding of negatively charged proteins.

The best obtained result of a western blot is through normalization of the measured band intensities. Normalization enables relative or absolute quantification by adjusting to variance in gel application and the transmission onto the membrane. This can be achieved by normalizing the band intensities to a reference protein or to total protein. The latter has been shown to produce enhanced sensitivity in combination with the Stain-free technology, compared to normalization to a reference gene, as well as to the traditional Coomassie Brilliant Blue- and Ponceau stains (Gürtler et al., 2013; Rivero-Gutiérrez, Anzola, Martínez-Augustin, & de Medina, 2014; Welsh et al., 2020). The Stain-free technology make use of an irreversible tryptophane formation in proteins by a trihalo compound implemented in the acrylamide gel. Henceforth, the protein fluorescence by exposure to ultraviolet light. Normalisation to total protein is often favoured to normalisation by reference protein. A reference protein must be validated and its expression unchanged by the experimental conditions. Additionally, the reference protein's quantity must be in line with the detection method's linear dynamic range (Gürtler et al., 2013).

3.7.1 Sodium Dodecylsulphate-Polyacrylamide Gel Electrophoresis

10 µg sample were mixed 1:1 with sample buffer and boiled at 95 °C for 5 minutes. The sample mixtures were subsequently separated on a 4-15% polyacrylamide-gel. Sodium Dodecyl Sulphate-Polyacrylamide Gel Electrophoresis (SDS-PAGE) was carried out in a Mini-PROTEAN Tetra Cell at constant current at 200 V for 45 minutes in 1x Running buffer with Precision Plus Protein™ Western C™ Standard. After electrophoresis the gel was imaged using the ChemiDoc™ XRS+ System with the Stain-free gel application, 1 minute activation, and 1 second exposure.

3.7.2 Western Blot

A PVDF-membrane was activated by brief exposure to methanol while the pads were soaked in 1x Transfer buffer. Following, a blotting sandwich was assembled by pads, PVDF-membrane, gel, and pads from anode to cathode, respectively. Any intralayer bubbles were removed and the cassette placed in the Trans-Blot® Turbo™ for transfer. The Trans-Blot® Turbo™ was ran at default settings at 1.32A/22V for 7 minutes. Subsequently, the membrane was washed 3x10 minutes in washing buffer before being blocked in 5% blocking buffer for 2 hours in room temperature whilst shaken. Following an additional 3x10 minutes wash, the

membrane was covered in 5% blocking buffer with monoclonal anti CYP1a1-antibody (concentration/1:500) and Precision Protein StrepTactin-HRP Conjugate (concentration/1:10 000) added. The membrane and blocking buffer mix incubated for 1 hour at room temperature whilst shaken, followed by incubation at 4 °C over night. The following morning the membrane was washed 5x10 minutes to adequately remove unbound antibodies. The ECL Prime Western Blotting Detection Reagents were mixed 1:1 and added to the membrane for 3 minutes while covered. The blot was imaged using the ChemiDoc™ XRS+ System whit optimalization for intense bands, with no application, 1 minute activation, and 1 second exposure. An additional picture of the gel was taken to verify the transfer efficiency to the membrane.

3.7.3 Total Protein Normalization

All Western Blots were normalized to total protein in the ImageLab software. The program's lane- and band function outlined the wells in the depicted membrane as well as the wanted band. The corresponding Stain-free gel was chosen as normalization channel and the normalization lane set to the intensity of all proteins in the corresponding lane. Furthermore, the lane containing the protein standard was marked as such by the Molecular Weight Analysis Tool, in order to exclude its intensity from the normalization calculations.

3.8 Primer Design

Target specific primers for qPCR were designed using the National Centre for Biotechnology Information (NCBI) primer-BLAST submission form. The target gene's accession number (NCBI, 11622) was entered in the PCR Template section followed by a primer-BLAST. The primers' location was assessed in regard to the differences between genetic sequences in murine and humane AhR. Furthermore, three primers were picked and included for further assessment and amplification efficiency.

3.9 One-Step RT-PCR

The designed primers amplification was verified using the OneStep RT-PCR kit followed by agarose gel electrophoresis. Firstly, the primers were diluted in 50 µM TE-buffer and vortexed 3x30 seconds. Subsequent, a reaction solution was mixed, and PCR performed, both as specified in 2.8.1. The PCR product was run at an 1% agarose gel, made from 1 g agarose, 100 ml TAE buffer and 2.5 µl GelRed. The agarose was dissolved by rapid heating, cooled to approximately 50 °C and casted. 10x BlueJuice loading buffer was added to the PCR product

in a 1:4 relationship. GelPilot 50 bp was used as protein standard. Electrophoresis was carried out at 80 V for approximately 1 hour. Finally, the gel was depicted using the ChemiDoc™ XRS+ system with the GelRed application.

3.10 RNA EXTRACTION FORM CELL CULTURE

Pre-incubated HEPA 1-6 and TM4 cells with FA or BSA were seeded at concentrations of 15 000 and 16 700 cells per cm^2, respectively. As the cultures reached a confluence of approximately 80%, they were exposed to 100 nM TCDD and harvested the following day (~24 hours). RNA from cells were extracted using the RNeasy® Plus Mini Kit according to the manufacturers protocol. Cells were adequately washed with PBS and disrupted using 600 µl of Buffer RLT Plus. The buffer is a highly denaturing guanidine-isothiocyanate containing buffer, which ensures isolation of intact RNA due to the immediate inhibition of RNases. Homogenization was done by adding the lysate directly to a QIAshredder spin column and centrifuged for 2 minutes at maximum speed. Selective removal of genomic DNA was done by adding the homogenate to a gDNA eliminator spin column and centrifuged for 30 seconds at 8 000 x g. Following, ethanol was added 1:1 to the flow-through providing the appropriate RNA binding conditions. Consequently, total RNA binds to the membrane and is rinsed from contaminants as the flow-through passes through the RNeasy spin column. The membrane was washed as stated by the manufacturer using the RW1 and RPE buffer. The membrane was additionally centrifuged at maximum speed for 1 minute, to ensure elimination of residual flow-through or RPE buffer, containing ethanol. Thus, preventing interference in downstream analysis. Finally, RNA was eluted in 50 µl RNase-free water. The eluate was additionally re-eluted to retrieve a higher final RNA concentration.

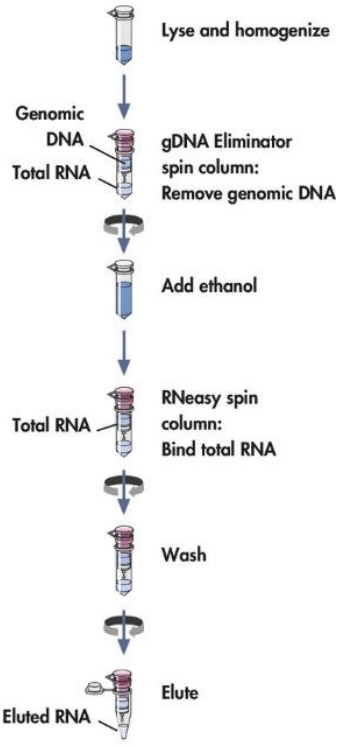

Figure 4: RNeasy Plus workflow. Adapted from qiagen.com, RNeasy Plus Kits, Total RNA extraction protocol: RNeasy Plus procedure.

3.11 RNA EXTRACTION FROM TISSUE

Approximately 100 mg tissue were cut while on dry ice and transferred to prefilled Precylls homogenization tubes with 750 µl Qiazol and four ceramic beads. Qiazol, a monophasic solution of phenol and guanidine thiocyanate, facilitates tissue lysis and inhibits RNases. The samples were homogenized using the Precellys® 24 homogenizer at 6 000 rpm for 3x15

seconds and incubated for 5 minutes at room temperature. 150 µl chloroform was added to the homogenate and given a quick shake, followed by a 3-minute incubation at room temperature and centrifugation for 15 minutes at 12 000 x g at 4 °C. The addition of chloroform leads to a separation into aqueous and organic phases by centrifugation, segregating RNA from proteins, DNA, and other impurities within the sample. Hence, the RNA partitions to the upper aqueous phase, leaving DNA in the interphase and proteins in the bottom organic phase. Furthermore, the RNA was transferred to a new tube and purified using a BioRobot EZ1 and the EZ1 RNA Tissue Mini Kit according to the manufacturers protocol. Briefly, RNA binds to magnetic beads where the RNA is washed and purified, before finally being eluted in RNase-free water. Furthermore, all samples were DNase treated to prevent DNA contamination in downstream analysis.

3.12 RNA Quality and Quantity

The RNAs concentration and purity was assessed spectrophotometrically by Nanodrop™ 1000. As molecules absorb light at distinct wavelengths, a sample's absorption spectra can be utilized to calculate its RNA concentration and assess its purity. RNA absorbs light at 260 nm, hence, by assessing its light-absorption ratio to DNA's at 280 nm (260nm/280nm) and proteins' at 230 nm (260nm/230nm) the sample's purity can be evaluated. A 260/280 ratio at ~1.8-2.0 is considered as optimal, whereas a 260/230 ratio at ≥1.7 indicates a non-contaminated sample from protein and phenol. As to avoid RNA degradation all samples were kept on ice during the analysis, using 2 µl of each sample.

A spectrophotometric analysis does not however present information regarding RNA's integrity. Hence, twelve samples were randomly selected and analysed using the BioAnalyzer and RNA 6000 Nano LabChip Kit according to the manufacturers protocol. Briefly, RNA Nano dye and gel-matrix were mixed and centrifuged at 13 000 x g for 10 minutes. Meanwhile, the chosen RNA-samples were denatured at 70 °C for 2 minutes. Next, an RNA 6000 Nano Chip was placed in the Chip priming Station and the gel-mix, RNA marker, and RNA ladder was added to their respective wells. The chip was vortexed at 2 400 rpm for 1 minute and analysed in the BioAnalyzer. For each sample the analysis produced an RNA integrity number (RIN) and an electropherogram, making it possible to assess the RNA integrity. RIN is an objective metric of total RNA quality, where 1 and 10 is the equivalent to completely degraded- and highly intact RNA, respectively.

3.13 PRECIPITATION OF RNA

Samples with a 260/230 ratio < 1.7 were precipitated to assure removal of impurities. This was done to prevent interference in sensitive downstream analysis, such as qPCR. By adding sodium acetate (0.1:1) to the applicable samples, ribose's negative charge is neutralised making the molecule less hydrophilic. Further, absolute ethanol is added (2.5:1) hence precipitating RNA in the solution. Subsequently, all samples were incubated at -80 °C over night and centrifuged at 12 000 x g for 10 minutes at 4 °C. RNA sediments in the pellet and the supernatant was thus carefully discarded. Residual impurities were removed by washing with 75% ethanol. Furthermore, the solution was centrifuged anew, and the ethanol was discarded as thoroughly as possible. After drying the pellet, it was resuspended in RNase-free water.

3.14 REAL TIME QUANTITATIVE PCR

Real-time quantitative PCR (qPCR) enables measurement and reliable detection of products generated through the PCR cycles by fluorescence. An example of fluorescence in qPCR is the implementation of SYBR® Green, a cyanine dye. The dye binds proportionally to the minor grove of double-stranded DNA as amplicons accumulate. Hence, by measuring the fluorescence emission of the dye, DNA amplicons can be monitored in real time (Wilson & Walker, 2010).

A prerequisite for accurate gene expression in qPCR data is normalization to a reference gene, normally a housekeeping gene within the system. The ideal reference gene should not be affected by experimental conditions and its expression level similar to the target gene. It has, however, been reported considerable variation in housekeeping gene expression (Vandesompele et al., 2002). Hence, the geNorm algorithm utilizing multiple reference genes was used in the present study, allowing a more accurate gene-expression profiling (Vandesompele et al., 2002). GeNorm is an algorithm that determines the most stable reference genes in a given sample panel from a set of tested candidate reference genes. Based on the geometric mean of a user-defined number of reference genes, a gene expression normalization factor may thus be generated for each sample (Vandesompele et al., 2002).

3.14.1 CDNA SYNTHESIS

RNA was diluted in RNase-free water to a final concentration of 50 ng/µl (± 5.0%). A stock solution, consisting of all RNA samples, was used to make a standard curve required for downstream analysis. The standard curve was made by a six serial dilution starting at 100 ng/µl

to a final 3.125 ng/µl. Subsequently, a reaction mix was prepared as specified in 2.8.2, and 40 µl solution per well was added to a 96-well cDNA plate. 500 ng of each RNA was added in duplicates alongside the standard curve being added in triplicates. In addition to the RNA samples, a non-amplification control and a non-template control were added to the cDNA plate. The controls constitute the same reaction solution, only being deprived of enzyme and a substitution of RNA with RNase-free water, respectively. The plate was centrifuged at 50 x g for 1 minute and cDNA synthesised in a T100 Thermal Cycler as specified in 2.8.2. Finally, cDNA was diluted 1:1 in dH_2O using the Biomek 4000 pipetting robot, followed by a 1 200 x g centrifugation for 1 minute and vortex at 1 500 rpm for 5 minutes.

3.14.2 qPCR

The reaction mix described in 2.8.3 was made for all primers. 8 µl reaction mix and 2 µl cDNA was added to a qPCR plate per well by the Biomek 4000 pipetting robot. The qPCR plate was directly centrifuged at 1 500 x g for 2 minutes. Next, RT-qPCR was carried out in a CFX96 Touch Real-Time PCR Detection System as specified in 2.8.3.

3.14.3 Data Analysis

qPCR data was first assessed in the CFX Maestro software, where primarily E-values were reviewed alongside R^2. E-values in the range of 90%-110% and an R^2 as close as possible to 1 provided the data for further analysis. All samples' cycle quantification (Cq) values were evaluated and a deviation percentage at 0.2 was set as intra-variation cut-off. Furthermore, a normalization factor was calculated based on the geometric mean of multiple reference genes (TBP, β-actin, calnexin, and eef1a1) by utilizing the geNorm software and algorithm. M-value cut-off was set as <1.5 for *in vivo* gene expression analysis, and M<2.5 for *in vitro* gene expression analysis. The difference in M-value cut-off was used due to methodological challenges and will be further discussed (5.1.1). β-actin was excluded for all testis tissue samples due to its substantially higher M value, thus lower stability, compared to the remaining control genes. Subsequently, the normalization factor was applied for all samples.

3.15 Statistical Analysis

Raw data was plotted and processed using Microsoft excel. Statistical calculations and figure creations were performed using GraphPad Prism 8. Unless otherwise stated, all statistical analyses were calculated by a tow-way analysis of variance (ANOVA) followed by a post hoc

Tukey's multiple comparisons test. All results are presented as mean with 95% confidential interval. Differences with a significance level at $p<0.05$ are illustrated by letters in the results.

The dose of the effective dose-response relationship between cell growth and TCDD exposure was confirmed using semi-log regression.

Factorial set up was designed for the *in vitro* and *in vivo* studies. A factorial design provides the possibility to test the effect of several variables simultaneously, as well as any interaction effect between the variables. Furthermore, a factorial design increases the statistical power without increasing the number of test animals.

4. RESULTS

4.1 ESTABLISHING CELL SEEDING- AND TCDD EXPOSURE CONCENTRATIONS

HEPA 1-6, TM4, and MLTC-1 were seeded at 15 000 cells per cm^2, 16 700 cells per cm^2, and 15 000 cells per cm^2, respectively. These cell concentrations were optimised through preliminary cell titrations. Furthermore, suitable TCDD concentrations were established by examining dose-response interactions in cell growth (Figure 5). Doses of 1 nM, 10 nM, and 100 nM TCDD were deemed suitable to study TCDD response with FA *in vitro*. Cell growth was decreased significantly from control (Ctr) to 0.1 nM TCDD ($p<0.05$) and continued to decline until 100 nM TCDD. However, changes in cell growth between 0.1 nM to 100 nM, did not show significant differences ($p>0.05$).

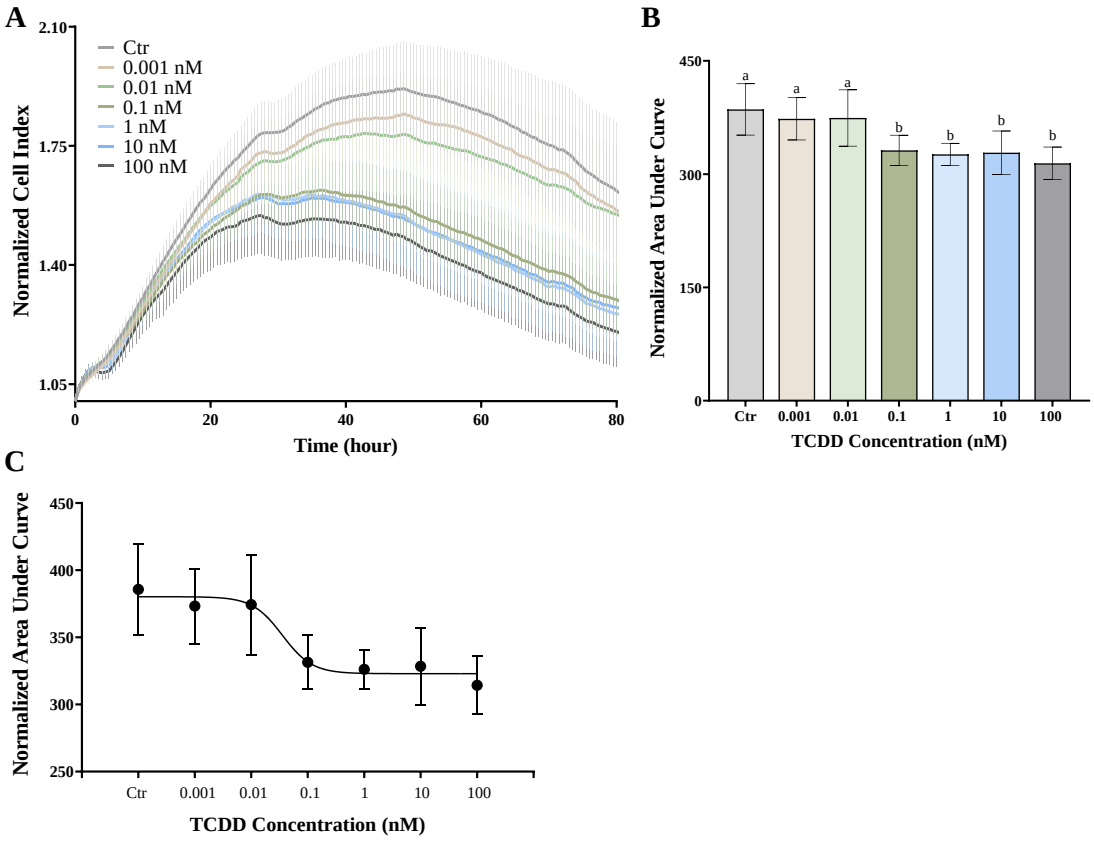

Figure 5: TCDD dose-response curve. (**A**) The normalized cell growth measurements are presented as mean impedance 80 hours after TCDD exposure ± SD (n=14). A significant decline in cell growth from ctr to 0.1 nM TCDD ($p<0.05$) is observed.. (**B**) Mean area under curve of normalized cell growth ± SD (n=14). Significant effects ($p<0.05$) of TCDD are shown using a bracket line and arrow indicating reduced cell growth. Differences in dose-response are denoted by small letters. (**C**) Semi-log regression visualising mean decline in cell growth ± SD as well as dose-response.

4.2 Differences in Cyp1a1 Expression by Cell Type

HEPA 1-6, MLTC-1 and TM4 cells were exposed to 100 nM TCDD prior to cell harvesting. Proteins were homogenised and SDS-PAGE performed. Separated proteins were transferred to a PVDF-membrane and Cyp1a1 was detected by monoclonal antibodies (Figure 6). The antibodies detected bands at various sizes in liver cells and testicular cells. HEPA 1-6 shows a prominent band at approximately 57 kDa in TCDD treated sample (100) and is the only sample showing this band throughout the membrane. Both MLTC-1 and TM4 show a band of approximately 70 kDa and 130 kDa, with MLTC-1 being more prominent than TM4. The same bands can vaguely be seen in un-treated and treated HEPA 1-6 sample, however, somewhat more prominent in its treated sample. Furthermore, a third vague band across all samples, treated and un-treated, at approximately 65 kDa was additionally observed in all cell lines.

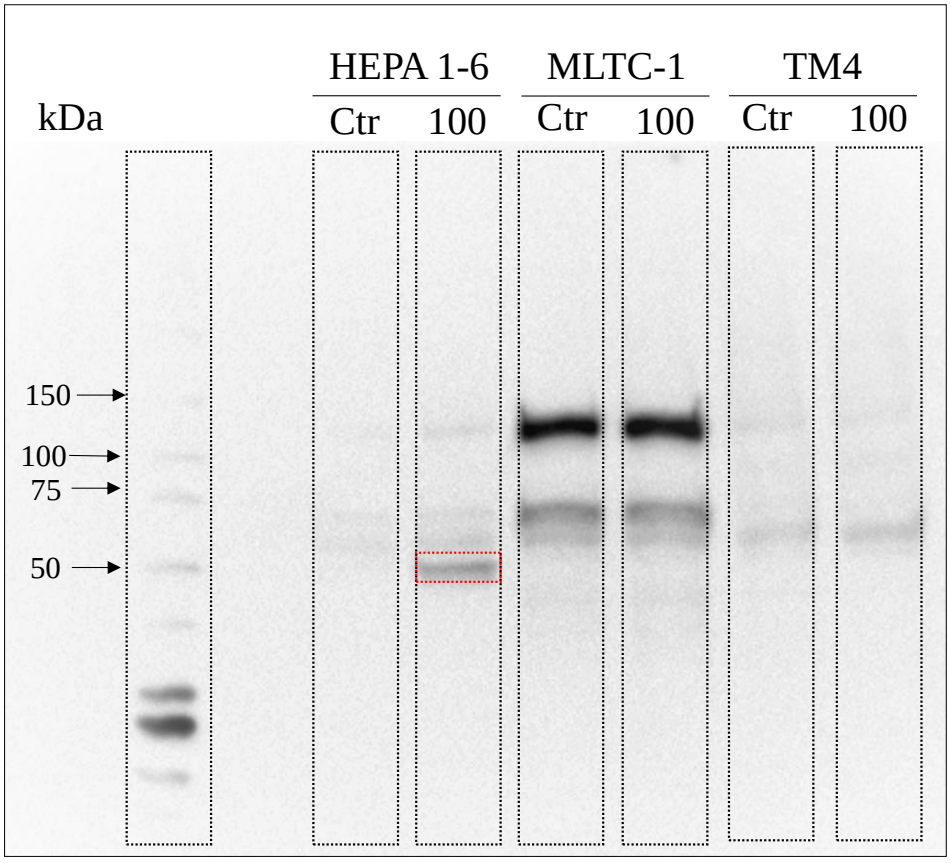

Figure 6: Western Blot of HEPA 1-6, MLTC-1 and TM4 cells with and without exposure to TCDD. Homogenised cells exposed to 100 nM TCDD were separated by SDS-PAGE and transferred to a PVDF-membrane. Cyp1a1 was detected by incubating the membrane in monoclonal Anti-CYP1a1 Antibody. Protein size was compared to the protein standard Precision Plus Protein WesternC Standard. All cell lines are represented by control (Ctr) and cells exposed to 100 nM TCDD (100). Overall, HEPA 1-6 treated with 100 nM show a prominent band at ~50 kDa (outlined by a red rectangle) but not in control. MLTC-1 and TM4 show the same bands in control and treated sample at ~70 kDa. MLTC-1 shows an additional band at ~130 kDa in both its samples.

4.3 Interaction of Fatty Acids with TCDD Toxicity on Cell Growth

HEPA 1-6 cells pre-incubated with n-3 fatty acids were exposed to TCDD to investigate potential interaction between FA and TCDD toxicity (Figure 7). Cells pre-incubated with DHA showed the overall highest cell growth, both in control and during TCDD exposure. Consistently for both FA and BSA, cell growth decreased as TCDD concentration gradually increased. Cells pre-incubated with EPA, however, showed a temporary stagnation in cell growth, or flattened curve, in TCDD exposed cells after five hours. No difference in cell growth across TCDD concentrations was observed, as the viability at 1 nM – 100 nM were the same. However, approximately 30 hours after TCDD exposure a modest difference in cell growth was observed, with doses of 1 nM and 10 nM showing increasing and decreasing cell viability, respectively. The same trend was observed in BSA-incubated cells, differing with doses of 1 nM and 100 nM showing the greatest and poorest cell viability, respectively. Over time, the modest difference in cell growth with doses of 10 nM and 100 nM TCDD, diminishes.

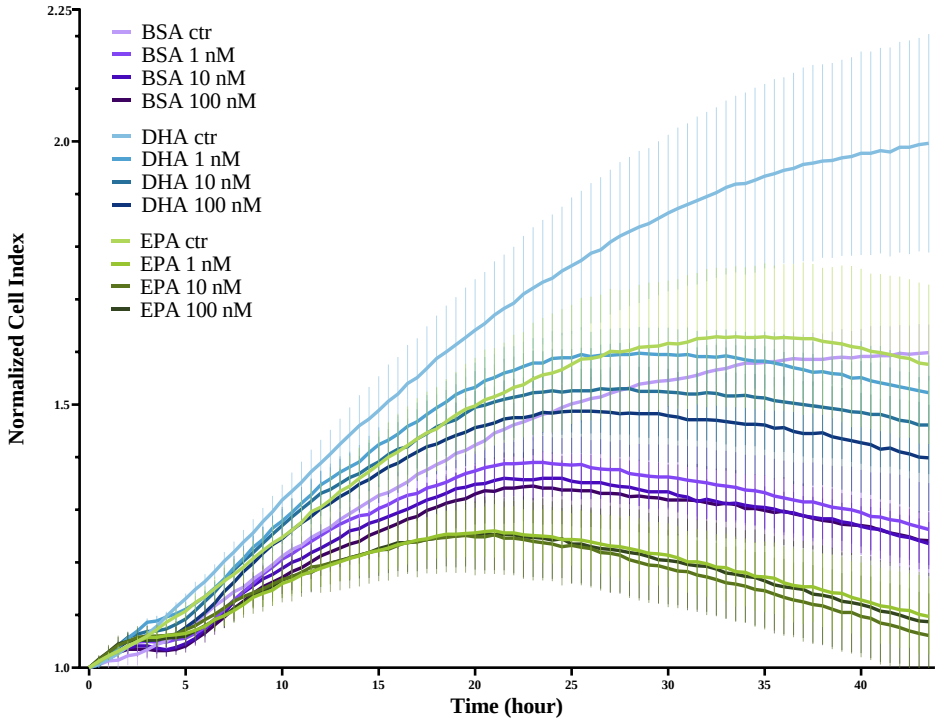

Figure 7: Interaction of fatty acids with TCDD exposure on HEPA 1-6 cell viability. Mean cell growth ± SD (n=8) measured using the xCelligence assay. In combination with FA, cells' impedance was monitored during TCDD exposure with doses of 1 nM, 10 nM, and 100 nM. The colour purple, blue, and green represents cells pre-incubated in BSA, DHA, or EPA, respectively. Furthermore, the gradient of the colours depicts the various TCDD concentrations utilized, where increasing TCDD concentration is indicated by a stronger gradient.

Based on the TCDD-FA interaction on cell growth presented in Figure 7, the area under curve (AUC) was extracted to further analyse the all-time combined exposure (Figure 8A). When examining AUC, a main interaction effect between TCDD and FA was observed ($p=0.009$), as well as differences within both FAs and TCDD concentrations ($p<0.05$). DHA showed the overall highest cell proliferation in both treated and un-treated samples. Henceforth, AUCs were normalized to control to emphasize the differences by FA interaction with TCDD exposure at different doses (Figure 8B). Based on delta mean AUC, cells preincubated with EPA showed the overall poorest cell viability at all TCDD concentrations when exposed. Furthermore, compared to BSA pre-incubated cells, both EPA- and DHA-incubated cells showed reduced cell growth ($p<0.05$). TCDD toxicity, however, is only significant at 1 nM compared to 100 nM TCDD ($p<0.05$). Cells pre-incubated with DHA did not show any significant difference compared to BSA, until 100 nM TCDD ($p<0.05$), nor a significant difference across all TCDD concentrations within its own group ($p>0.05$). The same intergroup-trend was observed for EPA-incubated cells ($p>0.05$), however, a significant difference compared to BSA was observed for all TCDD concentrations ($p<0.05$).

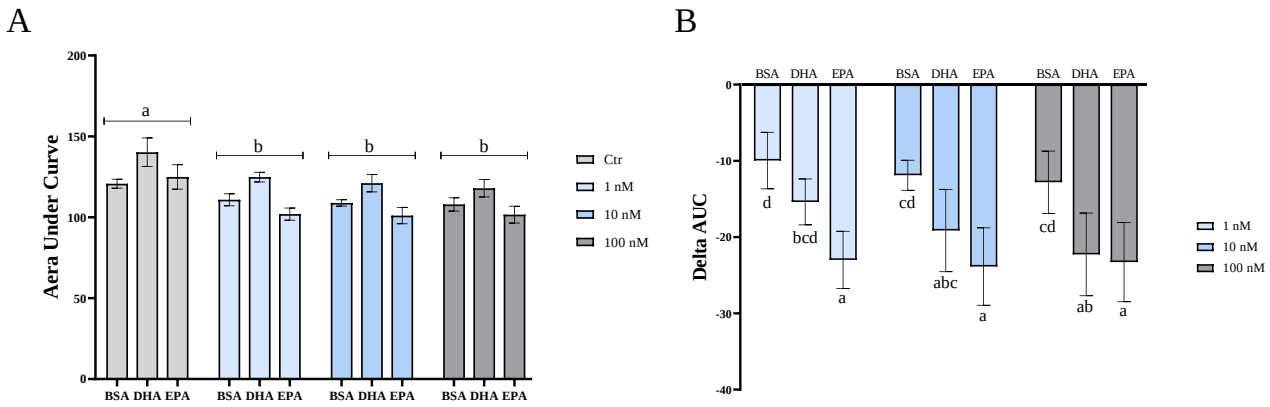

Figure 8: Area under curve of TCDD interaction with fatty acids in HEPA 1-6 cells. (**A**) Mean area under curve of cell growth ± SD (n=8). TCDD significantly reduced cell growth ($p<0.05$), also showing a significant main interaction of TCDD and FA ($p<0.05$). Significant main TCDD effect ($p<0.05$) is denoted by small letters. (**B**) Difference in mean AUC after normalization to control ± SD (n=8). Each FA's or BSA's AUC control was subtracted from their respective AUC of all TCDD exposure concentrations. Significant differences ($p<0.05$) are shown by small letters.

4.4 CYP1a1 EXPRESSION *IN VITRO*

HEPA 1-6 cells co-exposed to TCDD and marine n-3 fatty acids were further studied at protein expression level, more precisely, by the expression of Cyp1a1. Separated proteins from cells pre-incubated with FA were transferred to a PVDF-membrane and Cyp1a1 was detected by monoclonal antibodies (Figure 9). All groups were exposed to 1 nM and 10 nM TCDD, and all showed a prominent band at approximately 57 kDa (highlighted in red). The control (Ctr) samples, which had not been exposed to TCDD, did not show this band.

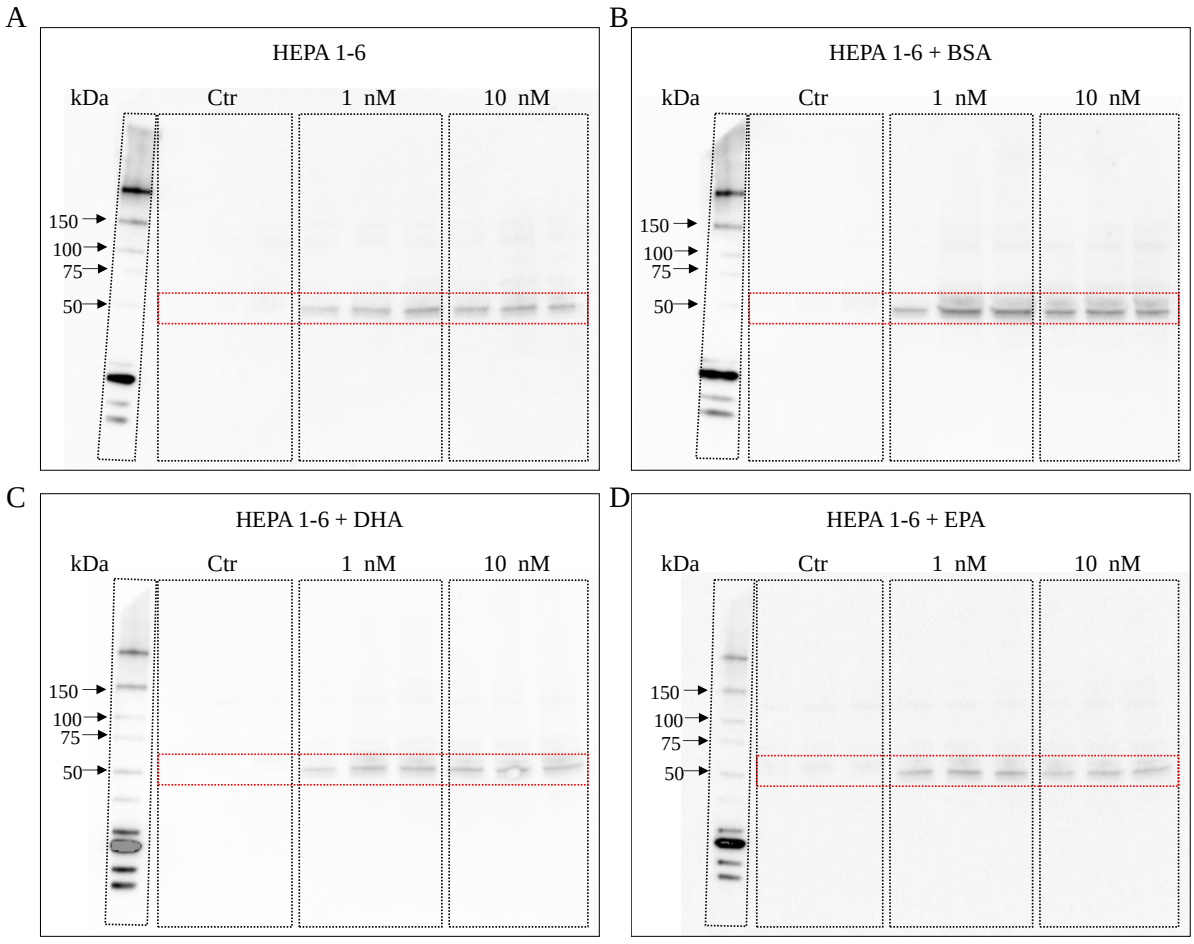

Figure 9: Western Blot of HEPA 1-6 cells co-exposed to marine n-3 fatty acids with and without TCDD. Cells without (**A**) and with pre-incubation with BSA (**B**), DHA (**C**), or EPA (**D**) were exposed to 1 nM or 10 nM TCDD. Homogenised cells were separated by SDS-PAGE and transferred to a PVDF-membrane. Cyp1a1 was detected by incubating the membrane in monoclonal Anti-CYP1a1 Antibody. Protein size was compared to the protein standard Precision Plus Protein WesternC Standard. All groups are represented by control (Ctr) and cells exposed to 1 nM or 10 nM TCDD.

Since the band intensities from all groups are separated to distinct membranes, they cannot directly be compared to study changes in TCDD toxicity in cells co-cultured with FA. To try to make such a comparison possible, a band detected from the protein standard (150 kDa) was

designated as normalization channel for each membrane (Figure 10). The band showed a uniform intensity throughout all membranes and was therefore selected as normalization channel. The normalized band intensities showed no difference of significance in Cyp1a1 expression between 1 nM and 10 nM TCDD in neither group ($p>0.05$), except for EPA-incubated cells ($p<0.05$). Furthermore, the band intensities corresponding to cells pre-incubated in DHA clearly stand out compared to all band intensities.

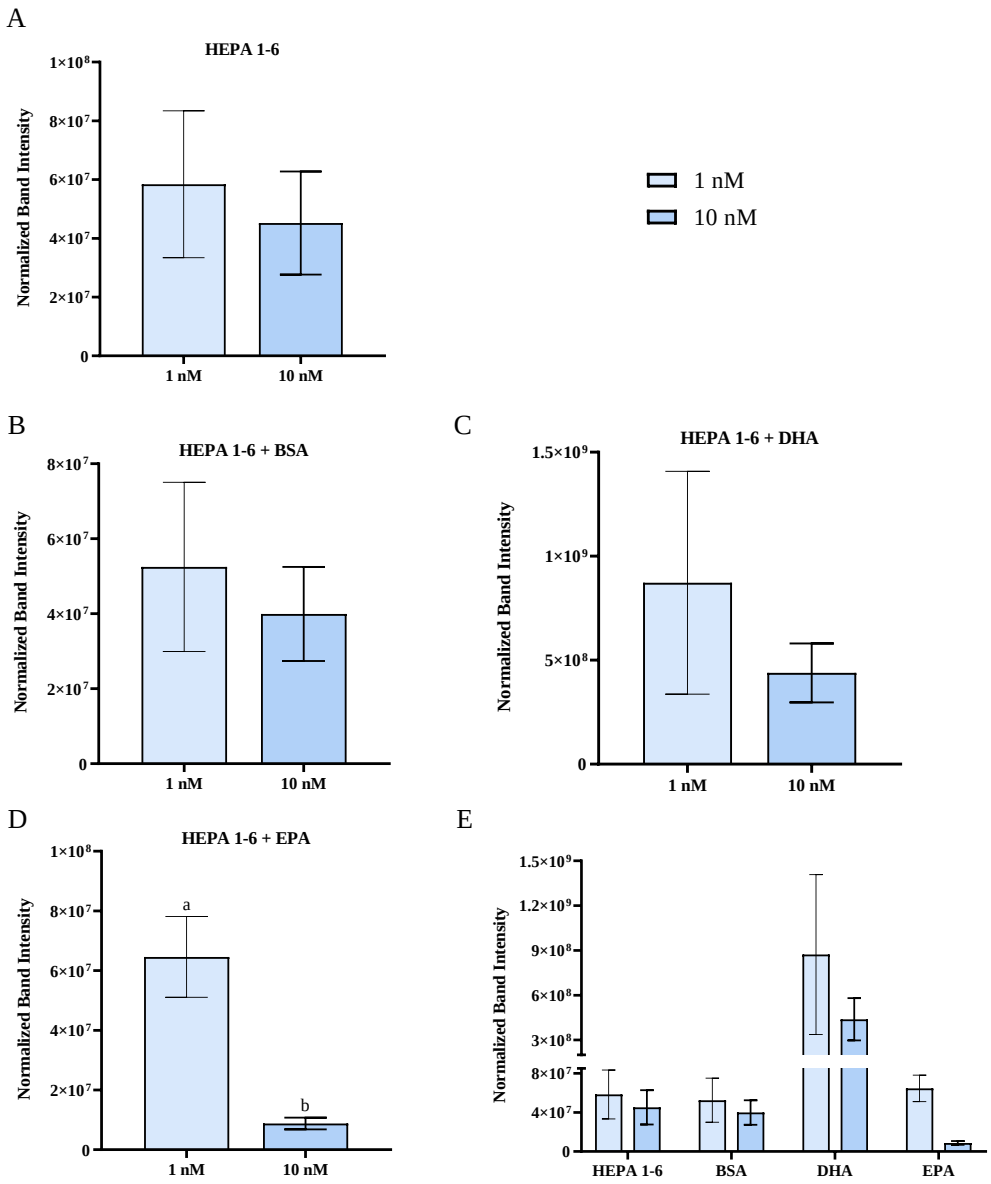

Figure 10: Normalized Western blot band intensities for HEPA 1-6 cells co-exposed with n-3 fatty acids and TCDD. Mean band intensity ± SD (n=3). HEPA 1-6 cells without (A) and with pre-incubation with BSA (B), DHA (C), or EPA (D) were exposed to 1 nM or 10 nM TCDD. **E**. All band intensities plotted in one graph, visualising the intensities in relation to one another. A significant difference between 1 nM and 10 nM TCDD was not observed for any groups ($p>0.05$), except for cells pre-incubated with EPA ($p<0.05$) (denoted by small letters). All control (Ctr) samples showed no band intensity and are therefore not presented in the figure.

4.5 PROTEIN EXPRESSION *IN VIVO*

Liver- and testicular tissue form male C57BL/6J mice modified with human Ahr were studied for Cyp1a1 expression *in vivo*. Homogenised liver- and testicular tissue were separated by SDS-PAGE and transferred to a PVDF-membrane. Cyp1a1 was detected by monoclonal antibodies (Figure 11). A prominent band at approximately 130 kDa and a subtle band at approximately 70 kDa were observed in both tissues for all groups. Furthermore, a third band at approximately 65 kDa was observed in testicular tissue for all groups. Though various bands were observed, neither were at 57 kDa, which is the predicted size of Cyp1a1.

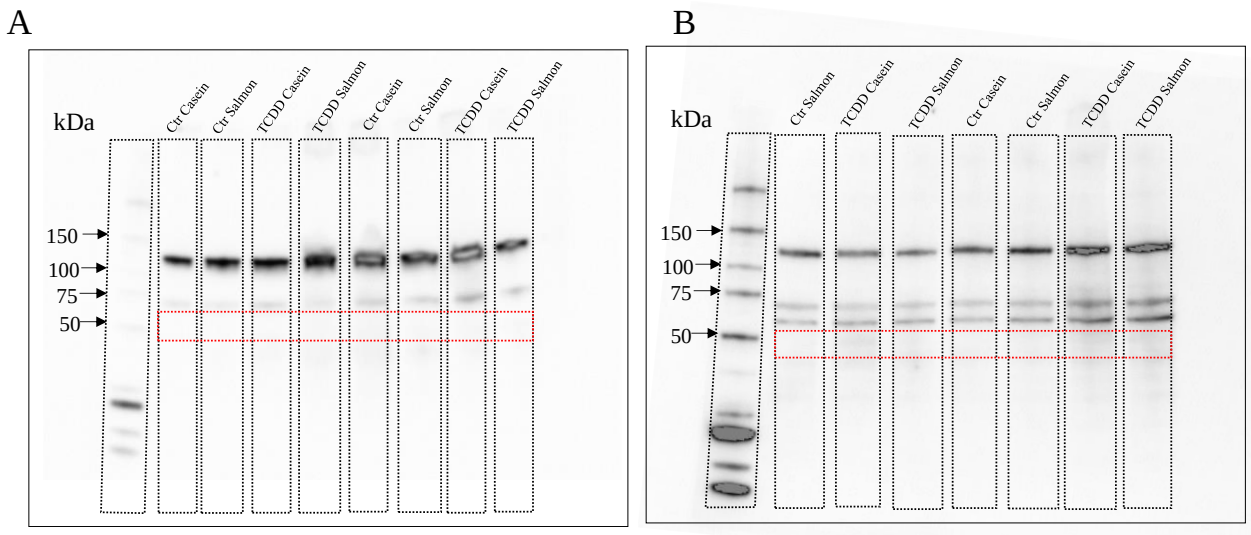

Figure 11: Representative western blot of liver (A) and testicular (B) tissue from C57BL/6J male mice. Mice were exposed to TCDD through dietary administration by casein (Ctr Casein), FA (Ctr Salmon), TCDD (TCDD Casein), or salmon filet (TCDD Salmon). Cyp1a1 was detected by incubating the membrane in monoclonal Anti-CYP1a1 Antibody. Protein size was compared to the protein standard Precision Plus Protein WesternC Standard. Both tissues showed a prominent band at ~130 kDa and a subtle band at ~70 kDa for all groups. Testicular tissue showed an additional band at ~65 kDa for all groups. A band at 57 kDa (highlighted in red), however, was not observed for any of the tissues.

4.6 VALIDATION OF AhR PRIMERS

The amplification efficiency of the newly designed AhR primers were evaluated using one-step RT-PCR and gel electrophoresis. One of the three proposed primers showed a prominent band of around 100 kDa. Consequently, because the expected product size of 97 kDa was observed and no primer dimerization was discovered, this primer pair was chosen for gene expression analysis by qPCR. The remaining primer pairs had previously been verified and used for qPCR analysis in-house.

4.7 GENE REGULATION BY TCDD INTERACTIONS WITH FATTY ACIDS *IN VITRO*

A pilot study examining relative gene regulation *in vitro* was performed due to low cell numbers and time constraints. Group diversity was favoured to sample size (n) considering the indicative means of the relative gene expression analysis. Gene expression was normalized to the geometric mean of multiple reference genes (TBP, β-actin calnexin, and eef1a1) using the geNorm software and algorithm (M<2.5). Difference in relative gene expression was not observed in any of the FA groups, in neither HEPA 1-6 cells (Figure 12) nor TM4 cells (Figure 13). Furthermore, abnormal amplification efficiencies were observed in all samples.

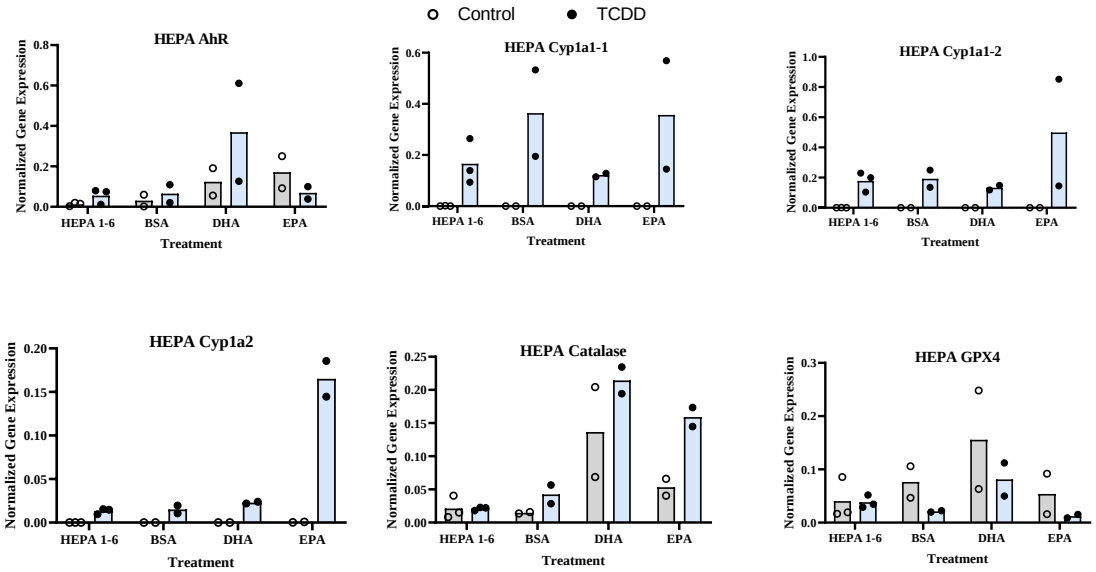

Figure 12: Normalized gene expression in HEPA 1-6 cells pre-incubated with FA in response to TCDD. Relative gene expression is shown by individual values and mean (n=3 for cells without FA, n=2 for cells pre-incubated with FA). Statistical analysis was not conducted due to the small sample size. Gene expression was detected by qPCR analysis. All samples were normalized to four reference genes using distinct Cq-values.

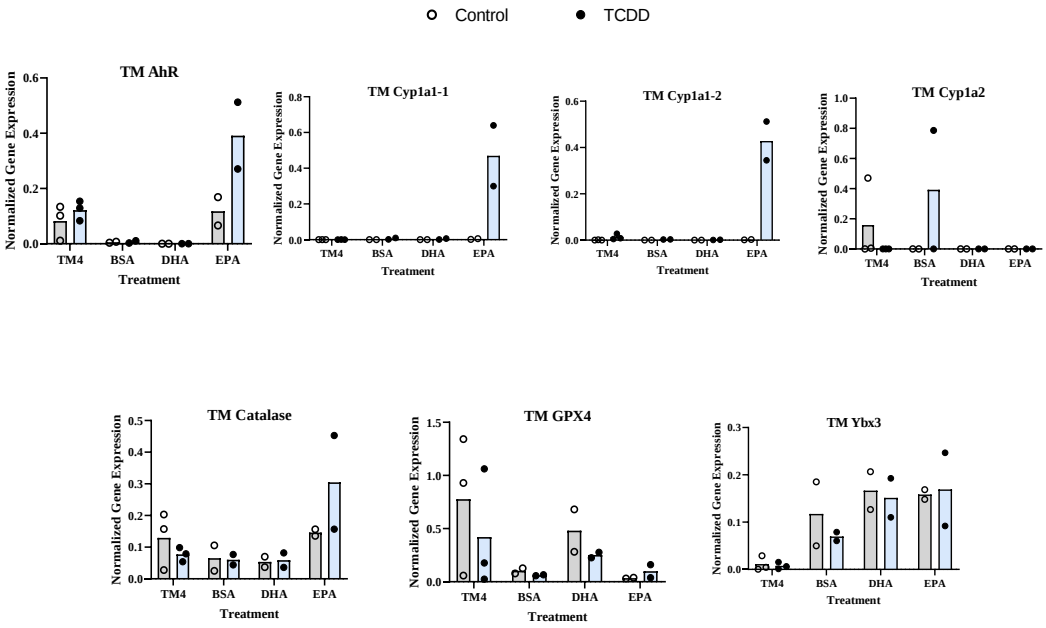

Figure 13: Normalized gene expression in TM4 cells pre-incubated with FA in response to TCDD. Relative gene expression is shown by individual values and mean (n=3 for cells without FA, n=2 for cells pre-incubated with FA). Statistical analysis was not conducted due to the small sample size. Gene expression was detected by qPCR analysis. All samples were normalized to four reference genes using distinct Cq-values.

4.8 GENE REGULATION BY TCDD INTERACTION WITH MARINE NUTRIENTS *IN VIVO*

Relative gene expression in response to TCDD and marine nutrients *in vivo* was included in this study. Gene regulation in male, human AhR modified C57BL/6J mice exposed to TCDD via control diet or salmon filet were studied. The geNorm software and algorithm were used to normalize relative gene expressions to the geometric mean of multiple reference genes (TBP, calnexin, and eef1a1). Relative gene expression in liver tissue did not show difference in gene transcription for any genes ($p>0.05$), with the exception being catalase (Figure 14). Catalase gene expression was significantly induced in mice fed salmon filet compared to mice fed casein ($p<0.05$). The same trend was observed in testicular tissue, where no significant differences were showed (Figure 15).

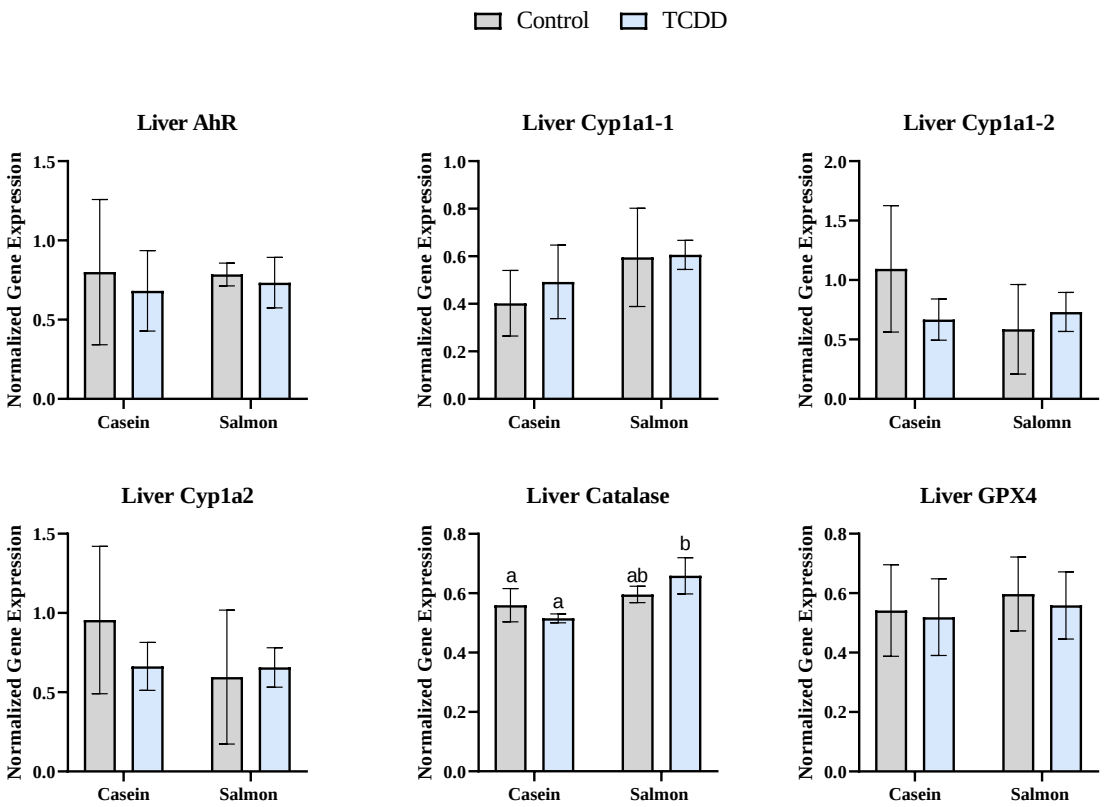

Figure 14: Normalized gene expression in liver tissue from human AhR modified male C57BL/6J mice fed with salmon. Mean normalized gene expression ± SD (n=8). Significant differences ($p<0.05$) are shown by small letters. No interaction effect was observed. Gene expression was detected by qPCR analysis. All samples were normalized to four reference genes using distinct Cq-values.

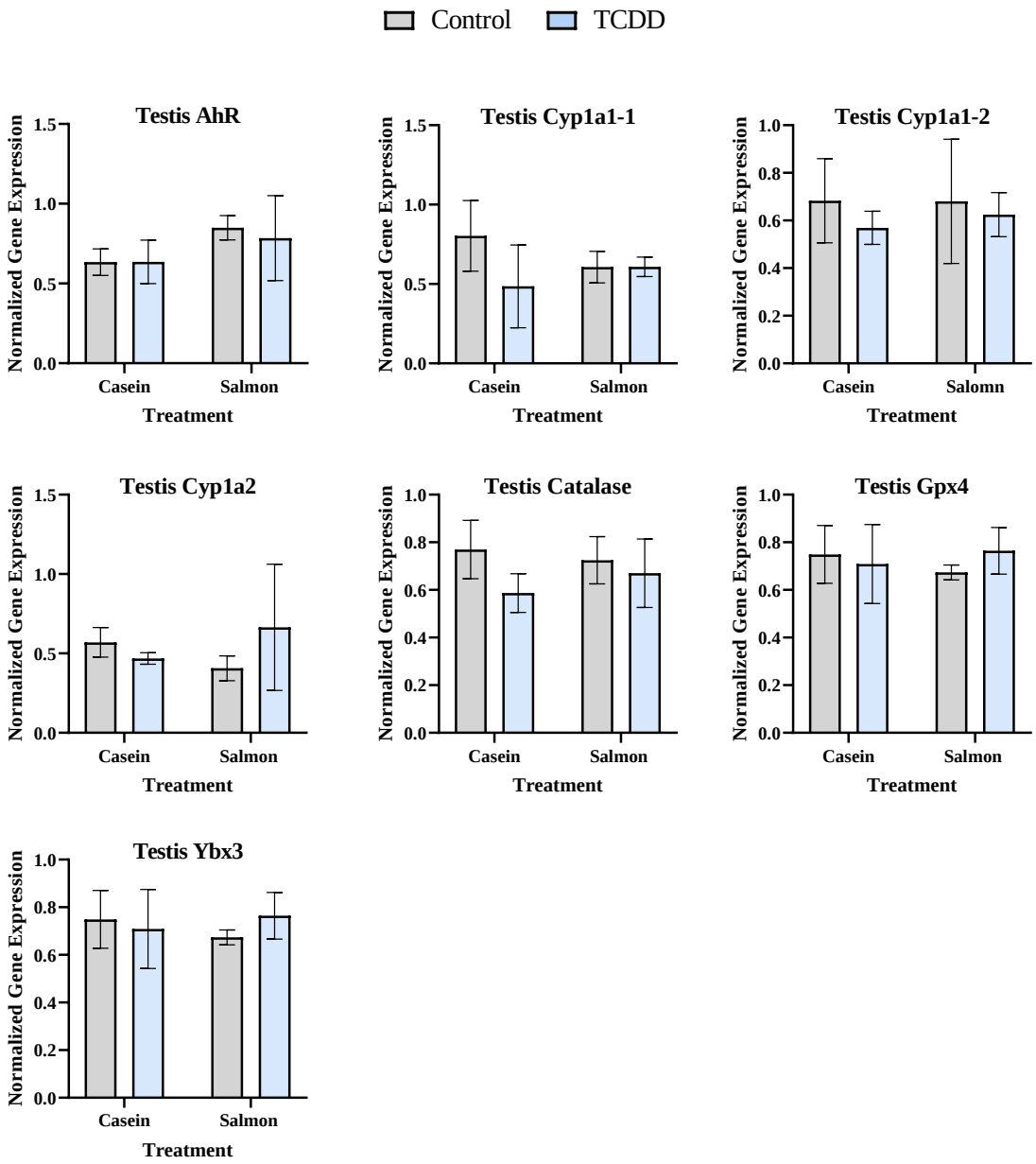

Figure 15: Normalized gene expression in testicular tissue from human AhR modified male C57BL/6J mice fed with salmon. Mean normalized gene expression ± SD (n=8). No interaction effect was observed. Gene expression was detected by qPCR analysis. All samples were normalized to three reference genes using distinct Cq-values.

5. DISCUSSION

In 2018 EFSA reduced the TWI by 7-fold for dioxin and dl-PCBs in foods. This 7-fold reduction in tolerable intake was based on the critical effects observed in semen quality and quantity. A longitudinal study investigating the negative effects in semen parameters by dioxin and dl-PCBs in Russian boys, was fundamental in EFSA's assessment. Furthermore, such observations have previously been seen in epidemiological studies, where dioxin and dl-PCBs seemed to impair sperm quantity and motility and delayed sexual maturation.

Fatty fish is a major contributor to dioxin exposure, but it is also an important source of valuable nutrients including n-3 fatty acids. The risk-benefit analyses performed by EFSA and VKM find that the health benefits obtained from fatty fish consumption surpass the hazardous effects of dioxin and dl-PCB. However, little is known about TCDD exposure and its interaction with FA, highlighting the demand of such investigations.

The interaction of TCDD with marine nutrients has previously been studied *in vivo* in male Wistar HAN rats, and human AhR modified male C57BL/6J mice (unpublished). Reproductive organs and mechanisms were studied but showed interactions of little significance. It was therefore desired to examine these effects *in vitro*, both to explore prospective differences as well as the *in vitro* effects itself. Aside from potential reproductive alterations, the co-exposure of TCDD and marine nutrients in liver was examined *in vivo* and *in vitro* seeing as the liver is a well-known target for the toxicological effects of TCDD.

5.1 DOES TCDD INDUCE A SIMILAR TOXIC RESPONSE IN TESTIS AS IN LIVER

TCDD toxicity is most commonly associated with its high-affinity binding to AhR and the subsequent expression of dioxin-responsive genes. The most well-known genes responding to TCDD is the enzymatic cytochrome P450 family (Schrenk, 1998). Cyp1a1 is one of the most studied and sensitive AhR regulated genes and have been observed highly expressed in mouse liver after TCDD exposure (Perdew, Murray, & Peters, 2010). AhR and Cyp1a1 activity is however not restricted to the liver and have been observed in several tissues (Perdew et al., 2010; Whitlock et al., 1997).

5.1.1 CYP1A1 EXPRESSION IN TESTICULAR CELL LINES COMPARED TO HEPATOCYTES

TCDD exposure to testis has resulted in various alterations and negatively impacted several testicular parameters (Elsayed et al., 2019). The mechanisms involved, however, are mostly unknown. As aforementioned, the prototypical AhR-regulation in response to TCDD is by Cyp1a1 gene transcription. Expression of Cyp1a1 can therefore indicate intracellular activation of AhR signalling pathways and toxicological response.

No Cyp1a1 protein expression was found in neither the TCDD treated Sertoli nor -Leydig cells in this study. Cyp1a1 deficiency was found using Western blot analysis and performed alongside protein extract from TCDD treated hepatocytes. The clear positive signal detected in hepatocytes makes it doubtful that the negative result was caused by sample preparation errors, or the sensitivity of the antibody used in this study. Furthermore, this result is supported by several experiments who also were unable to detect Cyp1a1 protein expression in TCDD treated Sertoli or -Leydig cells (Kapelyukh, Henderson, Scheer, Rode, & Wolf, 2019; Naville et al., 2011). Despite lack of Cyp1a1 protein expression in TCDD treated Sertoli or -Leydig cells, the Western blot analysis detected signal at various molecular weights. These bands were shown in both TCDD treated and un-treated sample, as well as in hepatocytes. This is interesting since a monoclonal antibody was used for Cyp1a1 detection and considering the clear Cyp1a1 protein signal detected only in TCDD treated hepatocytes. Monoclonal antibodies are made from one specific B-lymphocyte, thus recognising one antigen epitope solely. Hence, this specificity should exclude cross-binding and non-specific binding to supplementary proteins. However, it could be argued whether an excess of antibodies was present considering antibodies in excess may bind to targets of lower affinity resulting in non-specific antibody formation. This could be addressed by optimizing antibody concentration used during PVDF-membrane blocking by performing a titration study. Subsequently, such a study would optimize potential signal-to-background staining.

A modest constitutive expression of CYP1A1 and its substantial induction following exposure to TCDD is well established within toxicology and has been consistently identified in the livers of mice and rats (Moorthy, 2000; Walker et al., 1999; Zacharova et al., 2003). To current knowledge, few studies have examined the *in vivo* Cyp1a1 protein expression induced by TCDD in testis. Kapelyukh et al. (2019), however, examined Cyp1a1 and Cyp1a2 induction in response to TCDD in several tissues from mice modified with human Cyp1a1/1a2 and mice Cyp1a1/1a2 knockout. Using i.a. Western blot analysis, Kapelyukh et al. (2019) did not detect

Cyp1a1/1a2 in testicular tissue from any of the groups, despite positive signal in several other tissues. These results support the observation from *in vitro* analysis and emphasizes a Cyp1a1 deficiency in response to TCDD in testicular tissue and -cell lines. Based on these results, possible differences in biological mechanisms between *in vivo* and *in vitro* appear thus to be overcome.

It has previously been shown that there is not necessarily a clear connection between protein and gene expression (Lai, Wong, & Wong, 2005). In addition to Cyp1a1 protein expression in liver, TCDD exposure has also been observed to induce Cyp1a1 mRNA (Zhang et al., 2006). mRNA induction in response to TCDD exposure was also part of the present study. Furthermore, a consequence of, what is assumed, sample inhibitory contamination resulted in unreliable Cq values, and the results must thus be evaluated by uttermost caution. This fault is only applicable to qPCR results regarding *in vitro* samples, and is the cause for using different normalization cut-off values (M<2.5). Nevertheless, the gene expressions detected by qPCR analysis are discussed and used as indicative parameters to the cellular responses to TCDD exposure. Bearing the results' uncertainty in mind, in this study TCDD was found to induce Cyp1a1 mRNA expression in hepatocytes. Lai et al. (2005) reported a dose-dependent Cyp1a1 mRNA induction, despite not observing any expressed Cyp1a1 protein. Lai and colleagues (2005) observed a significant mRNA induction at the minimal dose of 2 pg/ml TCDD, indicating that Sertoli cells are highly responsive to TCDD exposure. Furthermore, they stipulated whether the sensitive induction of Cyp1a1 mRNA might be the attributor to the high susceptibility of male reproductive tissues to TCDD exposure (Lai et al., 2005). In this study however, Cyp1a1 mRNA was not observed in TCDD treated Sertoli cells, however, bearing the qPCR analysis' uncertainty in mind. Considering the TCDD dose dependency and Cyp1a1 mRNA sensitivity reported by Lai et al. it can be argued whether the obtained mRNA result in this study is truly indicative for the regulation of Cyp1a1 by TCDD toxicity. However, Lai and colleagues exposed Sertoli cells to a maximum dose of 2 000 pg/ml TCDD – the equivalent of approximately 10 nM TCDD. In this study, Sertoli cells were exposed to 100 nM TCDD prior to mRNA analysis. Thus, it can be postulated if the difference in Cyp1a1 mRNA expression is a response to exceeded cytotoxicity at 100 nM TCDD, mediating alternative toxicological cellular responses. This is however doubtful, especially considering no observed difference in cell viability by 10 nM and 100 nM TCDD in this study. Interestingly, Riberio et al. (2018) studied dysregulated pathways in human Sertoli cells exposed to TCDD, and reported of similar

Cyp1a1 expression. Notably however, reporting Cyp1a1 as not over-expressed in contrast to not expressed at all.

To current knowledge, few studies have investigated Cyp1a1 mRNA induction in Sertoli cell lines. Nonetheless, several studies have examined testicular TCDD toxicity *in vivo*. Interestingly, *in vivo* models report of non-significant Cyp1a1 mRNA expression in testis (Ohyama et al., 2007; Volz, Bencic, Hinton, Law, & Kullman, 2005). Hence, contradicting the *in vitro* dose dependent Cyp1a1 mRNA induction observed by Lie et al., whilst supporting the non-altered Cyp1a1 mRNA levels found by Riberio et al. (2018). Furthermore, it supports the indicative mRNA Cyp1a1 expression presented in this study. Conversely, Cyp1a1 gene expression in liver is observed in other studies (Huang et al., 2003; Santostefano et al., 1997). Differential Cyp1a1 expression in liver versus testis can be explained by tissue-specific promoters found within the Cyp1a1 gene. Specific gene-protomers allow transcriptional activation by AhR in response to its agonists in some tissues but not to others. Subsequently, transcriptional variation in AhR recruitment and histone modification could play a crucial role of Cyp1a1 expression in various tissues (Hankinson, 2005; R. T. Taylor, Wang, Hsu, & Hankinson, 2009). Expression by the AhR repressor (AhRR) have also been suggested as a possible explanation to Cyp1a1 deficiency in testis. Furthermore, AhRR is observed expressed at high levels in testis and at low levels in liver (Bernshausen, Jux, Esser, Abel, & Fritsche, 2006; Yamamoto et al., 2004). AhRR is proposed to compete with AhR in the formation of the AhR-ARNT dimer, subsequently supress AhR-mediated activity (Bernshausen et al., 2006; Tsuchiya, Nakajima, Itoh, Iwanari, & Yokoi, 2003). Although no correlation has been found between Cyp1a1 enzyme induction and AhR repressor levels, it is plausible that AhRR suppresses AhR-stimulated Cyp1a1 transcription in the testis (Hankinson, 2005; R. T. Taylor et al., 2009).

5.1.2 AhR's Role in Testicular TCDD Toxicity

Testis is comprised of numerous protective barriers and components. One of these adaptive mechanisms is AhR and its related gene battery (Beischlag, Morales, Hollingshead, & Perdew, 2008). Numerous experiments have shown reduced TCDD-mediated toxicity in AhR-knockout animals (Fernandez-Salguero, Hilbert, Rudikoff, Ward, & Gonzalez, 1996; Huang et al., 2003). Henceforth, it is generally established that TCDD-induced toxicity is mediated through AhR-pleiotropic pathways. Based on the lack of Cyp1a1 observed in testis the plausible AhR-alternative signalling pathways for TCDD-mediated toxicity is enhanced. Gene expression

analysis of TCDD exposed Sertoli cells revealed a modest increase of expressed AhR. The increased expression of AhR in testis has been reported in various studies as well as expression of AhRR (Magre et al., 2012). Considering the lack of Cyp1a1 expression the plausibility of alternative AhR pathways in testis is thus further supported.

AhR is a pleiotropic protein, and its effects are not restricted to the induction of Cyp1a1 in response to TCDD toxicity. Among AhR's many mechanisms, the protein is proposed to induce TCDD toxicity though the mediation of xanthine oxidoreductase. This enzymatic system comprises xanthine oxidase and xanthine dehydrogenase and are involved in the generation of reactive oxygen species (ROS). Antioxidant enzymes such as glutathione peroxidase and catalase constitute part of the defence system against generated ROS in Sertoli cells and mitochondria (Jin, Hong, Lee, Kang, & Han, 2008). Oxidative stress can be caused by an imbalance in the ROS- and antioxidant system. TCDD have shown to disturb this balance in mouse testis by decreasing enzymatic antioxidants and subsequently resulting in enhanced levels of ROS and reproductive abnormalities in male rats, causing reduced fertility (Gray Jr, Ostby, & Kelce, 1997). By qPCR analysis similar result were observed in this study by reduced antioxidant gene expression of *cat* and *gpx4* in Sertoli cells exposed to TCDD. These antioxidants are essential in homeostasis maintenance and are individually characterized. Catalase prevents cellular damage by metabolizing hydrogen peroxide to water and oxygen. Glutathione peroxidase 4 (Gpx4) is involved in the detoxification of lipid peroxides and, as the only member of the glutathione peroxidase family, can degrade hydroperoxides found in lipoproteins and complex lipids.

Analysing expressed genes in Sertoli cells also showed reduced levels after TCDD exposure in the *ybx3* gene. Y-box binding protein 3 (Ybx3) is pivotal in triggering the transformation of protamine, a protein sharing similar properties with histones, in post-meiotic male germ cells (Jin et al., 2008). Lai et al. (2005) reported of TCDD interference with Sertoli cell functions by inhibited gene expression of Mullerian inhibiting substance and induced gene expression of 17 beta-estradiol (E2). Reproductive functions, including spermatogenesis, sperm motility, and differentiation, are regulated by MIS and E2. Henceforth, the reduced *ybx3* expression observed in this study, accompanied by the findings of Lie et al. (2005), might be explained as possible mechanism for the negative impact of TCDD toxicity in sperm quality. However, considering the uncertainty encumbered in the gene expression results from this study, this statement can merely be stipulated.

Gene expressions were additionally investigated *in vivo* as part of the present study. No significant difference in neither *cat*, *gpx4* nor *ybx3* in testis tissue were observed. This however might not fully provide the full picture of TCDD's impact on testicular and sperm parameters. The mice included in the animal study were chronic exposed to TCDD for 13 weeks and the aforementioned TCDD-induced alterations may have been present in the early stages of the study. However, as time has passed, some TCDD-induced alterations may have been overcome and homeostasis approximately restored. Though the antioxidant genes were downregulated they were not fully inhibited as some gene expression was obtained. Considering the ROS-antioxidant system is based on consecutively regulation for best maintaining the system's homeostasis, the constant presence of ROS can have maintained a persistent antioxidant gene expression. Hence, over time the concentration of transcribed antioxidants may have reached sufficient levels for supressing the oxidative state within the cells.

5.2 Does n-3 Fatty Acids Affect TCDD Toxicity

TCDD mediates toxic reactions through a variety of mechanisms and hence extensive effort has been deemed to determine its mode of action. However, little research has been devoted to alleviating TCDD toxicity and the possibility for diet with natural supplements to offer significant protection. DHA and EPA are essential n-3 fatty acids and are known to contribute to a variety of health benefits in humans. Risk-benefit analysis of fatty fish consumption rich in FA consistently concludes the benefits obtained by DHA and EPA outweighs the health impairments by dioxin exposure obtained from the same dietary source. Interestingly, few endeavours have been made to investigate the interaction of these compounds.

Considering the modest TCDD induced toxicity observed in testicular cell lines, the potential interaction of FA and TCDD was mostly examined in hepatocytes. However, Sertoli cells were partly included for the FA-TCDD interaction study due its pivotal role in male reproduction. Furthermore, Sertoli cells were co-exposed with FA and TCDD considering EFSA's TWI re-evaluation, and its fundament being based on semen parameters by dioxin and dl-PCBs.

5.2.1 TCDD Interaction with n-3 Fatty Acids on Cell Viability

Cell viability can be assessed as an indirect measure of the cellular response to a foreign substance (Cell Signaling Technology, 2022). In the present study, hepatocyte's cellular

viability to TCDD-FA exposure was measured using the non-invasive impedance assay. DHA and EPA appeared to stimulate overall cell growth. Furthermore, exposing hepatocytes enriched with FA to TCDD showed a significant decrease in cell growth based on the observed cell-stagnation. To the best of my knowledge few studies have examined the possible interactions between TCDD and FA regarding cell viability. However, a previous study examining the FA metabolism in response to TCDD showed a decline in FA-levels upon exposure. The study also found a distinct decline in FA levels for FA comprising shorter carbon-chains (Jennen et al., 2011). Based on the theory of FA-metabolism and the observed cell viability to TCDD exposure, the cell growth stagnation might be explained based on cellular malnutrition. This can be further supported by the difference between cell growth in DHA- and EPA-incubated cells. DHA is a fatty acid comprised by a 22-carbon long chain and EPA by a 20-carbon long chain. Furthermore, DHA contains one additional double carbon bond compared to EPA, which i.a. provides resistance and stabilisation. Hence, the difference is modest, however, adequate to mediate a plausible distinct TCDD-toxicity response measured by cell growth. BSA vehicle-incubated cells also showed a decline in cell growth upon TCDD exposure, the decline in cell growth can thus not be only explained by loss of n-3 fatty acid nutrients. It might, however, rather be an indication as to why a difference in cell growth is observed between cells pre-incubated in DHA or EPA.

An interaction effect between FA and TCDD was observed. However, it was decided to exclude the interaction effects between TCDD and FA due to the allegedly elevated cell growth in DHA-incubated cells. The result was therefore normalized to control, compensating for AUC differences and to examine the obtained result with more accuracy.

5.2.2 Cyp1a1 Expression in n-3 Fatty Acid Enhanced Hepatocytes

TCDD mediates AhR activity and induces Cyp1a1 expression, which in turn can metabolize DHA and EPA. Studies have reported of increased Cyp epoxidated and hydroxylated metabolites in response to TCDD (Yang, Solaimani, Dong, Hammock, & Hankinson, 2013).

A dietary study investigating potential preventative effects of FA to TCDD toxicity in male mice reported attenuated Cyp1a1 mRNA expression by TCDD exposure. Furthermore, the observed Cyp1a1 expression was induced without significantly affecting AhR expression. The attenuated Cyp1a1 levels was however restricted to some tissues, excluding the liver (Wiest et al., 2016). In the present study qPCR- and Western blot analysis was used to examine the

expression of Cyp1a1 in response to TCDD in FA-rich cells. Cyp1a1 gene expression analysis in DHA-incubated hepatocytes did not show altered induction compared to the control samples, who were not pre-incubated with FA. In cells pre-incubated with EPA, it was observed overall enhanced Cyp1a1 expression. The same trend was additionally observed for Cyp1a2 gene expression. Thus, contradicting the Cyp1a1 mRNA expression in EPA-enriched liver presented by Wiest et al. (2016), who observed no altered Cyp1a1 gene expression compared to their control sample. However, the *in vitro* qPCR result's uncertainty must be considered. The obtained *in vivo* gene expression results, however, are not encumbered by this uncertainty and show similar results as presented by Wiest et al. (2016). Hence, the *in vitro* Cyp1a1 gene expression observed in this study may ultimately not be suited to provide a true indication of Cyp1a1 regulation in response to TCDD exposure.

In vitro Cyp1a1 protein expression was significantly enhanced by TCDD exposure with DHA-incubated hepatocytes compared to the other groups but did not show a significant difference across TCDD concentrations. Conversely, hepatocytes pre-incubated with EPA showed attenuated Cyp1a1 expression at 10 nM TCDD. However, methodological challenges may be responsible for the differences in detected Cyp1a1 expression. Due to the several PVDF-membranes used the obtained Cyp1a1 intensities cannot be used directly to study changes in TCDD toxicity. Precise normalization and quantification derived from different experiments on a traditional one-dimensional western blot are imprecise and poses numerous challenges (S. C. Taylor & Posch, 2014). The normalized intensities are thus semi-quantitative considering the many steps and possibilities for loss of protein and detected signal. Henceforth, the induced Cy1a1 proteins observed in the present study must be carefully interpreted and may be due to experimental errors. In the present study Cyp1a1 was also sought investigated *in vivo*. Interestingly, Cyp1a1 was not detected in liver tissue in neither group of TCDD exposed mice. Cyp1a1 expression and its increasing levels in response to TCDD in liver is well established in toxicology (Moorthy, 2000; Welsh et al., 2020; Zacharova et al., 2003). Hence the observed lack of Cyp1a1 in liver presented in this study is controversial. It could be postulated whether post-translational modifications and unknown alterations occurring in an *in vivo* system are responsible for these results. This can be supported by the Western blot analysis where various intensities were observed at higher molecular weights. Moreover, this is rather unlikely considering the well documented Cyp1a1 expression at 57 kDa. However, a possible return to homeostasis as a result of *in vivo* chronic TCDD exposure can also describe the lack of Cyp1a1 expression.

5.2.3 TCDD-Mediated Oxidative Stress in n-3 Fatty Acid incubated Cells

As previously discussed, TCDD toxicity involves duplex mechanisms and is not only restricted to the induction of Cyp1a1. Knowledge of the various TCDD-toxicity mechanisms combined with the beneficial n-3 fatty acids have gradually increased trough the recent years. TCDD has been shown to increase levels of several eicosanoids, mostly by lipoxygenase (Yang et al., 2013). Lipoxygenase belongs to a family of nonheme iron-containing enzymes and catalyse the deoxygenation of n-3 fatty acids subsequently yielding the essential signalling molecules eicosanoid (Miranda-Bautista, Bañares, & Vaquero, 2017). However, the knowledge of possible interaction effects of TCDD with n-3 fatty acids regarding male reproduction are slim.

As previously discussed, reduced antioxidant gene expression of *cat* and *gpx4* was observed in Sertoli cells exposed to TCDD. Furthermore, studies have previously reported of reduced antioxidant gene expressions in hepatocytes also, in response to TCDD (Kono & Fridovich, 1982). Reduced *cat* and *gpx4* expression were however not observed in this study but is likely a consequence of the uncertainty encumbered in the qPCR results. The results' invalidity is further supported by the reported detrimental effect of TCDD in hepatic tissue. TCDD has been reported to disrupt the functional integrity of hepatocytes and is therefore known to be responsible for the carcinogenic effects associated with oxidative DNA damage (Hung, Huang, Sava, Blagodarsky, & Hong, 2006). Moreover, studies implementing EPA have reported of increased mRNA expression of antioxidant genes in rat hepatocytes. The study reported that EPA reduced cellular level of ROS by maintaining elevated antioxidant enzyme levels (Kim & Chung, 2007). Similar results were allegedly observed in this study as both DHA- and EPA-incubated hepatocytes showed increased *cat* gene expression. Interestingly, increased *cat* gene expression was also observed in EPA-incubated Sertoli cells. This could possibly suggest that 3-n fatty acids protect antioxidant gene expression and subsequently attenuate TCDD-mediated toxicity in testis.

In vivo gene expressions in response to TCDD combined with marine nutrients were also examined in this study. No difference in neither *gpx4* nor *ybx3* gene expression were observed in liver from salmon fed mice. Gene expression of *cat* in salmon fed mice, however, were elevated. Notably, the difference was observed when comparing control- and TCDD samples from mice fed on the casein-control diet, and not the control within the samples own group. Similar observations were found in testis tissue. However, the result of the animal study reported of increased body- and liver weight (unpublished) which have been associated with

morphological alterations in response to TCDD toxicity (Lamb et al., 2016). It may therefore be stipulated whether possible TCDD-induced responses have been re-regulated and have over time returned to their normal state of function. Other mechanisms could also be involved, however considering the well-established regulatory system of ROS/antioxidant expression, the return to homeostasis may be likely.

6. CONCLUSION

The warrant to reveal TCDD's mode of action in male reproductive toxicity is persistent and are increasingly sought elucidated. Henceforth, part of this study was devoted to investigating the TCDD-mediated toxicity in testis. The result presented, did not reveal any induction of Cyp1a1 expression in Sertoli cells, nor in testicular tissue. Such an observation is not the first of its kind and is thus emphasizing the possibility for alternative TCDD-mediated mechanisms. Furthermore, reduced levels of antioxidant expression were observed and does therefore support the possibility for an alternative toxic mode of action. Interestingly, reduced antioxidant expression was not observed *in vivo*, highlighting the possibility for a regulated defence mechanism response. However, a possible return to homeostasis as a result to long time exposure must not be ignored.

N-3 fatty acids are pivotal nutritional supplements for mammals and have been suggested to protect against TCDD toxicity. In this present study, no interaction effects of n-3 fatty acids in TCDD toxicity were observed. This however can be explained by the discussed methodological challenges. Moreover, the allegedly increased antioxidant expression observed in n-3 fatty acids rich cells emphasize their role as a potential protector against TCDD-toxicity.

In conclusion, i) TCDD does not appear to induce a similar toxic response in testis as in liver due to the lack of Cyp1a1 induction. ii) TCDD toxicity in testis does however appear to be partly induced by AhR. Furthermore, based on the results presented, iii) it cannot be said with certainty that n-3 fatty acids reduce TCDD toxicity. It does however pose as a promising source for protecting against the impact of TCDD toxicity.

7. FUTURE PERSPECTIVES

Due to the methodological challenges that arose, *in vitro* qPCR analysis should be repeated. Additionally, considering the inability to compare Cyp1a1 detected proteins across several PVDF-membranes, one membrane could have been devoted to all groups. This would have provided a relative Cyp1a1 expression and indication of the quantity present in all groups, and to compare the groups to each other. Moreover, considering loading limitations, the Smart Protein Layer (SPL) technology provided by DyeAgnostics (Faden, Eschen-Lippold, & Dissmeyer, 2016) could have been used. The technology is based on fluorescent label of total protein detection and is combined with a sample-dependent bi-fluorescent standard. Henceforth, data derived from individual experiments can be compared.

The un-identified signals detected by western blot analysis in *in vivo* should be further examined. This could for example be done by chromatography, since the bands molecular weights have been established. Immobilized metal-affinity chromatography could have been a sufficient starting point due to the complex mixture within in the samples.

In the present study it was sought to examine oxidative stress in response to TCDD in established hepatocytes. HEPA 1-6 cells were transiently transfected with the reduction-oxidation sensitive green fluorescence protein (roGFP). Furthermore, the transfected cell cultures were exposed to various TCDD concentrations and H_2O_2 (positive control) at two distinct intervals. This was to investigate if a potential difference in acute and long-term exposure could be observed. However, this part of the study was excluded as detection difficulties arose along with time constraints. Henceforth, the detection method should be optimized, and the experiment repeated.

To further elucidate the mechanism of TCDD-mediated toxicity in testis, the involvement of the remaining Cyp members could be a suitable target for investigation. Furthermore, AhR's pleiotropic functions, subsequently resulting in oxidative stress and inflammation should also be sought elucidated. Though no significant interaction effects between TCDD and n-3 fatty acids was observed in the present study, its potential role in defending the male reproductive system should be investigated. In this regard, oxidative stress and inflammatory mechanisms could also be suitable for further investigations.

REFERENCES

Agilent. (2022). Cellular Impedance Retrieved from https://www.agilent.com/en/technology/cellular-impedance

Alsabeeh, N., Chausse, B., Kakimoto, P. A., Kowaltowski, A. J., & Shirihai, O. (2018). Cell culture models of fatty acid overload: Problems and solutions. *Biochimica et biophysica acta. Molecular and cell biology of lipids, 1863*(2), 143-151. doi:10.1016/j.bbalip.2017.11.006

Assennato, G., Cervino, D., Emmett, E., Longo, G., & Merlo, F. (1989). Follow-up of subjects who developed chloracne following TCDD exposure at Seveso. *American Journal of Industrial Medicine, 16*(2), 119-125.

Aune, T. (2007). *Næringsmiddeltoksikologi: tilsetningsstoffer, miljøgifter og naturlige toksiner*: Høyskoleforl.

Bazinet, R. P., & Layé, S. (2014). Polyunsaturated fatty acids and their metabolites in brain function and disease. *Nature Reviews Neuroscience, 15*(12), 771-785.

Beischlag, T. V., Morales, J. L., Hollingshead, B. D., & Perdew, G. H. (2008). The aryl hydrocarbon receptor complex and the control of gene expression. *Critical Reviews™ in Eukaryotic Gene Expression, 18*(3).

Bernshausen, T., Jux, B., Esser, C., Abel, J., & Fritsche, E. (2006). Tissue distribution and function of the Aryl hydrocarbon receptor repressor (AhRR) in C57BL/6 and Aryl hydrocarbon receptor deficient mice. *Archives of toxicology, 80*(4), 206-211.

Bolann, B. J., Huber, S., Ruzzin, J., Brox, J., Huitfeldt, H. S., & Monsen, A.-L. B. (2017). Er miljøgifter i norsk kosthold skadelig for barn? *Tidsskrift for Den norske legeforening*.

Cell Signaling Technology. (2022). Synopsis of Cell Proliferation, Metabolic Status, and Cell Death. Retrieved from https://www.cellsignal.com/science-resources/cell-viability-and-survival

Chavan-Gautam, P., Rani, A., & Freeman, D. J. (2018). Chapter Six - Distribution of Fatty Acids and Lipids During Pregnancy. In G. S. Makowski (Ed.), *Advances in Clinical Chemistry* (Vol. 84, pp. 209-239): Elsevier.

Coelho, N., Pimpão, A., Correia, M., Rodrigues, T., Monteiro, E., Morello, J., & Pereira, S. (2021). Pharmacological blockage of the AHR-CYP1A1 axis: a call for in vivo evidence. *Journal of Molecular Medicine*, 1-29.

Dahman, Y. (2019). *Biomaterials Science and Technology: Fundamentals and Developments*: CRC Press.

Darlington, G. J., Bernhard, H. P., Miller, R. A., & Ruddle, F. H. (1980). Expression of liver phenotypes in cultured mouse hepatoma cells. *Journal of the National Cancer Institute, 64*(4), 809-819.

EFSA CONTAM, P., (EFSA Panel on Contaminants in the Food Chain),, Knutsen HK, Alexander J, B. L., Bignami M, Bruschweiler B, Ceccatelli S, Cottrill B, Dinovi M, Edler L, Grasl-Kraupp B, Hogstrand C, Nebbia CS, Oswald IP, Petersen A, Rose M, Roudot A-C, Schwerdtle T, Vleminckx C, Vollmer G, Wallace H, Furst P, Håkansson H, Halldorsson T, Lundebye A-K, Pohjanvirta R,, & Rylander L, S. A., van Loveren H, Waalkens-Berendsen I, Zeilmaker M, Binaglia M, Gomez Ruiz JA, Horvath Z, Christoph E, Ciccolallo L, Ramos Bordajandi L, Steinkellner H and Hoogenboom LR. (2018). Risk for animal and human health related to the presence of dioxins and dioxin-like PCBs in feed and food. *Efsa Journal, 16*(11), e05333. doi:https://doi.org/10.2903/j.efsa.2018.5333

El-Sabeawy, F., Wang, S., Overstreet, J., Miller, M., Lasley, B., & Enan, E. (1998). Treatment of rats during pubertal development with 2, 3, 7, 8-tetrachlorodibenzo-p-

dioxin alters both signaling kinase activities and epidermal growth factor receptor binding in the testis and the motility and acrosomal reaction of sperm. *Toxicology and Applied Pharmacology, 150*(2), 427-442.
Elsayed, H. Y. A., Borroto, E. T., Pliego, A. B., Dibarrat, J. A., Ramirez, F. R., Chagoyán, J. C. V., . . . Diaz-Albiter, H. (2019). Sperm Quality in Mouse After Exposure to Low Doses of TCDD. *Curr Top Med Chem, 19*(11), 931-943. doi:10.2174/1568026619666190520090132
Erickson, M. D. (2018). *Analytical chemistry of PCBs*: Routledge.
Erickson, M. D., & Kaley, R. G. (2011). Applications of polychlorinated biphenyls. *Environmental Science and Pollution Research, 18*(2), 135-151.
Ernst, R., Dombroski, D., & Merrick, J. (1990). Anaerobiosis, type 1 fimbriae, and growth phase are factors that affect invasion of HEp-2 cells by Salmonella typhimurium. *Infection and immunity, 58*(6), 2014-2016.
European Food Safety Authority. (2012). Dioxins and PCBs. Retrieved from https://www.efsa.europa.eu/en/topics/topic/dioxins-and-pcbs#eu-framework
Faden, F., Eschen-Lippold, L., & Dissmeyer, N. (2016). Normalized Quantitative Western Blotting Based on Standardized Fluorescent Labeling. *Methods Mol Biol, 1450*, 247-258. doi:10.1007/978-1-4939-3759-2_20
Feher, J. (2017). 2.1 - Cell Structure. In J. Feher (Ed.), *Quantitative Human Physiology (Second Edition)* (pp. 101-119). Boston: Academic Press.
Fernandez-Gonzalez, R., Yebra-Pimentel, I., Martinez-Carballo, E., & Simal-Gandara, J. (2015). A critical review about human exposure to polychlorinated dibenzo-p-dioxins (PCDDs), polychlorinated dibenzofurans (PCDFs) and polychlorinated biphenyls (PCBs) through foods. *Critical reviews in food science and nutrition, 55*(11), 1590-1617.
Fernandez-Salguero, P. M., Hilbert, D. M., Rudikoff, S., Ward, J. M., & Gonzalez, F. J. (1996). Aryl-hydrocarbon receptor-deficient mice are resistant to 2,3,7,8-tetrachlorodibenzo-p-dioxin-induced toxicity. *Toxicol Appl Pharmacol, 140*(1), 173-179. doi:10.1006/taap.1996.0210
Furue, M., Ishii, Y., Tsukimori, K., & Tsuji, G. (2021). Aryl Hydrocarbon Receptor and Dioxin-Related Health Hazards-Lessons from Yusho. *International journal of molecular sciences, 22*(2), 708. doi:10.3390/ijms22020708
Ghioni, C., Tocher, D. R., & Sargent, J. R. (1997). The effect of culture on morphology, lipid and fatty acid composition, and polyunsaturated fatty acid metabolism of rainbow trout (Oncorhynchus mykiss) skin cells. *Fish Physiology and Biochemistry, 16*(6), 499-513.
Gray Jr, L., Ostby, J., & Kelce, W. (1997). A dose–response analysis of the reproductive effects of a single gestational dose of 2, 3, 7, 8-tetrachlorodibenzo-p-dioxin in male Long Evans Hooded rat offspring. *Toxicology and Applied Pharmacology, 146*(1), 11-20.
Guo, X.-f., Tong, W.-f., Ruan, Y., Sinclair, A. J., & Li, D. (2020). Different metabolism of EPA, DPA and DHA in humans: A double-blind cross-over study. *Prostaglandins, Leukotrienes and Essential Fatty Acids, 158*, 102033. doi:https://doi.org/10.1016/j.plefa.2019.102033
Gürtler, A., Kunz, N., Gomolka, M., Hornhardt, S., Friedl, A. A., McDonald, K., . . . Posch, A. (2013). Stain-Free technology as a normalization tool in Western blot analysis. *Analytical biochemistry, 433*(2), 105-111.
Hankinson, O. (2005). Role of coactivators in transcriptional activation by the aryl hydrocarbon receptor. *Archives of biochemistry and biophysics, 433*(2), 379-386.

Haws, L. C., Su, S. H., Harris, M., DeVito, M. J., Walker, N. J., Farland, W. H., . . . Birnbaum, L. S. (2006). Development of a refined database of mammalian relative potency estimates for dioxin-like compounds. *Toxicological Sciences, 89*(1), 4-30.

Henley, D. V., Bellone, C. J., Williams, D. A., & Ruh, M. F. (2004). MAPK signaling pathways modulate IL-1β expression in human keratinocytes. *Archives of biochemistry and biophysics, 424*(1), 112-118.

Huang, P., Ceccatelli, S., Hoegberg, P., Sten Shi, T. J., Håkansson, H., & Rannug, A. (2003). TCDD-induced expression of Ah receptor responsive genes in the pituitary and brain of cellular retinol-binding protein (CRBP-I) knockout mice. *Toxicol Appl Pharmacol, 192*(3), 262-274. doi:10.1016/s0041-008x(03)00296-5

Hung, Y.-C., Huang, G. S., Sava, V. M., Blagodarsky, V. A., & Hong, M.-Y. (2006). Protective effects of tea melanin against 2, 3, 7, 8-tetrachlorodibenzo-p-dioxin-induced toxicity: antioxidant activity and aryl hydrocarbon receptor suppressive effect. *Biological and Pharmaceutical Bulletin, 29*(11), 2284-2291.

JECFA. (2002). *Evaluation of Certain Food Additives and Contaminants: Fifty-seventh Report of the Joint FAO/WHO Expert Committee on Food Additives* (Vol. 57): World Health Organization.

Jennen, D., Ruiz-Aracama, A., Magkoufopoulou, C., Peijnenburg, A., Lommen, A., van Delft, J., & Kleinjans, J. (2011). Integrating transcriptomics and metabonomics to unravel modes-of-action of 2, 3, 7, 8-tetrachlorodibenzo-p-dioxin (TCDD) in HepG2 cells. *BMC systems biology, 5*(1), 1-14.

Jensen, I.-J., Eilertsen, K.-E., Otnæs, C. H. A., Mæhre, H. K., & Elvevoll, E. O. (2020). An Update on the Content of Fatty Acids, Dioxins, PCBs and Heavy Metals in Farmed, Escaped and Wild Atlantic Salmon (Salmo salar L.) in Norway. *Foods, 9*(12), 1901. Retrieved from https://www.mdpi.com/2304-8158/9/12/1901

Jin, M. H., Hong, C. H., Lee, H. Y., Kang, H. J., & Han, S. W. (2008). Enhanced TGF-β1 is involved in 2, 3, 7, 8-tetrachlorodibenzo-p-dioxin (TCDD) induced oxidative stress in C57BL/6 mouse testis. *Toxicology Letters, 178*(3), 202-209.

Justino, C. I., Duarte, K. R., Freitas, A. C., Panteleitchouk, T. S., Duarte, A. C., & Rocha-Santos, T. A. (2016). Contaminants in aquaculture: Overview of analytical techniques for their determination. *TrAC Trends in Analytical Chemistry, 80*, 293-310.

Kanan, S., & Samara, F. (2018). Dioxins and furans: A review from chemical and environmental perspectives. *Trends in Environmental Analytical Chemistry, 17*, 1-13.

Kapelyukh, Y., Henderson, C. J., Scheer, N., Rode, A., & Wolf, C. R. (2019). Defining the contribution of CYP1A1 and CYP1A2 to drug metabolism using humanized CYP1A1/1A2 and Cyp1a1/Cyp1a2 knockout mice. *Drug Metabolism and Disposition, 47*(8), 907-918.

Kim, Y. J., & Chung, H. Y. (2007). Antioxidative and anti-inflammatory actions of docosahexaenoic acid and eicosapentaenoic acid in renal epithelial cells and macrophages. *Journal of medicinal food, 10*(2), 225-231.

Kimbrough, R. D., & Jensen, A. A. (2012). *Halogenated biphenyls, terphenyls, naphthalenes, dibenzodioxins and related products*: Elsevier.

Kono, Y., & Fridovich, I. (1982). Superoxide radical inhibits catalase. *Journal of Biological Chemistry, 257*(10), 5751-5754.

Kulkarni, P. S., Crespo, J. G., & Afonso, C. A. (2008). Dioxins sources and current remediation technologies—a review. *Environment international, 34*(1), 139-153.

Lai, K. P., Wong, M. H., & Wong, C. K. C. (2005). Effects of TCDD in modulating the expression of Sertoli cell secretory products and markers for cell–cell interaction. *Toxicology, 206*(1), 111-123. doi:https://doi.org/10.1016/j.tox.2004.07.002

Lamb, C. L., Cholico, G. N., Pu, X., Hagler, G. D., Cornell, K. A., & Mitchell, K. A. (2016). 2,3,7,8-Tetrachlorodibenzo-p-dioxin (TCDD) increases necroinflammation and hepatic stellate cell activation but does not exacerbate experimental liver fibrosis in mice. *Toxicol Appl Pharmacol, 311*, 42-51. doi:10.1016/j.taap.2016.09.025

Long, W. P., Pray-Grant, M., Tsai, J. C., & Perdew, G. H. (1998). Protein kinase C activity is required for aryl hydrocarbon receptor pathway-mediated signal transduction. *Molecular pharmacology, 53*(4), 691-700.

Magre, S., Rebourcet, D., Ishaq, M., Wargnier, R., Debard, C., Meugnier, E., . . . Le Magueresse-Battistoni, B. (2012). Gender differences in transcriptional signature of developing rat testes and ovaries following embryonic exposure to 2, 3, 7, 8-TCDD. *PloS one, 7*(7), e40306.

Marlowe, J. L., & Puga, A. (2005). Aryl hydrocarbon receptor, cell cycle regulation, toxicity, and tumorigenesis. *Journal of cellular biochemistry, 96*(6), 1174-1184.

Matfier, J. P. (1980). Establishment and Characterization of Two Distinct Mouse Testicular Epithelial Cell Line. *Biology of Reproduction, 23*(1), 243-252. doi:10.1095/biolreprod23.1.243

Mínguez-Alarcón, L., Sergeyev, O., Burns, J. S., Williams, P. L., Lee, M. M., Korrick, S. A., . . . Hauser, R. (2017). A Longitudinal Study of Peripubertal Serum Organochlorine Concentrations and Semen Parameters in Young Men: The Russian Children’s Study. *Environmental Health Perspectives, 125*(3), 460-466. doi:doi:10.1289/EHP25

Miranda-Bautista, J., Bañares, R., & Vaquero, J. (2017). Chapter 1 - The Gastrointestinal System: Anatomy and Sources of Oxidative Stress. In J. Gracia-Sancho & J. Salvadó (Eds.), *Gastrointestinal Tissue* (pp. 3-20): Academic Press.

Mocarelli, P., Gerthoux, P. M., Ferrari, E., Patterson Jr, D. G., Kieszak, S. M., Brambilla, P., . . . Carreri, V. (2000). Paternal concentrations of dioxin and sex ratio of offspring. *The Lancet, 355*(9218), 1858-1863.

Mocarelli, P., Gerthoux, P. M., Patterson Jr, D. G., Milani, S., Limonta, G., Bertona, M., . . . Crespi, C. (2008). Dioxin exposure, from infancy through puberty, produces endocrine disruption and affects human semen quality. *Environmental health perspectives, 116*(1), 70-77.

Moorthy, B. (2000). Persistent expression of 3-methylcholanthrene-inducible cytochromes P4501A in rat hepatic and extrahepatic tissues. *Journal of Pharmacology and Experimental Therapeutics, 294*(1), 313-322.

Moutinho, V., Kingham, T., & D'Angelica, M. (2017). Blumgart's Surgery of the Liver, Biliary Tract, and Pancreas JARNAGIN, WILLIAM R. Philadelphia: Elsevier Saunders, 6th Edition. 2017 PART 7 Hepatic Disease / Section II. Neoplastic / D. Treatment - Nonresectional 98D. Cryotherapy and ethanol injection. In (pp. PART 7 Hepatic Disease / Section II. Neoplastic / D. Treatment-Nonresectional 98D).

Mozaffarian, D., & Rimm, E. B. (2006). Fish Intake, Contaminants, and Human HealthEvaluating the Risks and the Benefits. *JAMA, 296*(15), 1885-1899. doi:10.1001/jama.296.15.1885

Naville, D., Rebourcet, D., Chauvin, M.-A., Vega, N., Jalabert, A., Vigier, M., . . . Le Magueresse-Battistoni, B. (2011). Direct and indirect impact of 2,3,7,8-tetrachlorodibenzo-p-dioxin (TCDD) on adult mouse Leydig cells: An in vitro study. *Toxicology Letters, 207*(3), 251-257. doi:https://doi.org/10.1016/j.toxlet.2011.09.019

Ohyama, K., Ohta, M., Sano, T., Sato, K., Nakagomi, Y., Shimura, Y., & Yamano, Y. (2007). Maternal exposure of low dose of TCDD modulates the expression of estrogen receptor subunits of male gonads in offspring. *Journal of veterinary medical science, 69*(6), 619-625.

Perdew, G. H., Murray, I. A., & Peters, J. M. (2010). 1.17 - Xenobiotic Receptor-Mediated Toxicity. In C. A. McQueen (Ed.), *Comprehensive Toxicology (Second Edition)* (pp. 361-388). Oxford: Elsevier.

Pereira, M. d. S. (2004). Polychlorinated dibenzo-p-dioxins (PCDD), dibenzofurans (PCDF) and polychlorinated biphenyls (PCB): main sources, environmental behaviour and risk to man and biota. *Química Nova, 27*, 934-943.

Petrulis, J. R., & Perdew, G. H. (2002). The role of chaperone proteins in the aryl hydrocarbon receptor core complex. *Chemico-biological interactions, 141*(1-2), 25-40.

Pohjanvirta, R., & Tuomisto, J. (1994). Short-term toxicity of 2,3,7,8-tetrachlorodibenzo-p-dioxin in laboratory animals: effects, mechanisms, and animal models. *Pharmacol Rev, 46*(4), 483-549.

Rebois, R. V. (1982). Establishment of gonadotropin-responsive murine leydig tumor cell line. *J Cell Biol, 94*(1), 70-76. doi:10.1083/jcb.94.1.70

Ribeiro, M. A., Estill, M. S., Fernandez, G. J., Moraes, L. N., Krawetz, S. A., & Scarano, W. R. (2018). Integrative transcriptome and microRNome analysis identifies dysregulated pathways in human Sertoli cells exposed to TCDD. *Toxicology, 409*, 112-118.

Rivero-Gutiérrez, B., Anzola, A., Martínez-Augustin, O., & de Medina, F. S. (2014). Stain-free detection as loading control alternative to Ponceau and housekeeping protein immunodetection in Western blotting. *Analytical biochemistry, 467*, 1-3.

Santostefano, M., Wang, X., DeVito, M., Richardson, V., Ross, D., & Birnbaum, L. (1997). Multiple tissue pharmacokinetic analysis of TCDD-induced biochemical responses. *Organohalogen Compd, 34*, 19-24.

Schmidt, E. B., Arnesen, H., de Caterina, R., Rasmussen, L. H., & Kristensen, S. D. (2005). Marine n-3 polyunsaturated fatty acids and coronary heart disease: Part I. Background, epidemiology, animal data, effects on risk factors and safety. *Thrombosis research, 115*(3), 163-170.

Schrenk, D. (1998). Impact of dioxin-type induction of drug-metabolizing enzymes on the metabolism of endo-and xenobiotics. *Biochemical pharmacology, 55*(8), 1155-1162.

Singh, K. P., Casado, F. L., Opanashuk, L. A., & Gasiewicz, T. A. (2009). The aryl hydrocarbon receptor has a normal function in the regulation of hematopoietic and other stem/progenitor cell populations. *Biochemical pharmacology, 77*(4), 577-587.

Skåre, J. U., Brantsæter, A. L., Frøyland, L., Hemre, G. I., Knutsen, H. K., Lillegaard, I. T. L., . . . Hjeltnes, B. (2014). Benefit-risk assessment of fish and fish products in the Norwegian diet–an update. Opinion of the Scientific Steering Committee of the Norwegian Scientific Committee for Food Safety. *VKM Report*.

Sorg, O. (2014). AhR signalling and dioxin toxicity. *Toxicology Letters, 230*(2), 225-233. doi:https://doi.org/10.1016/j.toxlet.2013.10.039

Spector, A. A. (1999). Essentiality of fatty acids. *Lipids, 34*(1), S1-S3.

Suzuki, G., Nakano, M., & Nakano, S. (2005). Distribution of PCDDs/PCDFs and Co-PCBs in human maternal blood, cord blood, placenta, milk, and adipose tissue: dioxins showing high toxic equivalency factor accumulate in the placenta. *Bioscience, biotechnology, and biochemistry, 69*(10), 1836-1847.

Swanson, D., Block, R., & Mousa, S. A. (2012). Omega-3 fatty acids EPA and DHA: health benefits throughout life. *Advances in nutrition, 3*(1), 1-7.

Taylor, R. T., Wang, F., Hsu, E. L., & Hankinson, O. (2009). Roles of coactivator proteins in dioxin induction of CYP1A1 and CYP1B1 in human breast cancer cells. *Toxicological Sciences, 107*(1), 1-8.

Taylor, S. C., & Posch, A. (2014). The design of a quantitative western blot experiment. *BioMed research international, 2014*.

Thermo Fisher Scienific. (2022). Pierce™ 660nm Protein Assay Reagent. Retrieved from https://www.thermofisher.com/order/catalog/product/22660?msclkid=d46ab390ce5a11ecb8391e232bbffe56

Thiess, A., Frentzel-Beyme, R., & Link, R. (1982). Mortality study of persons exposed to dioxin in a trichlorophenol-process accident that occurred in the BASF AG on November 17, 1953. *American Journal of Industrial Medicine, 3*(2), 179-189.

Tian, Y., Rabson, A. B., & Gallo, M. A. (2002). Ah receptor and NF-κB interactions: mechanisms and physiological implications. *Chemico-biological interactions, 141*(1-2), 97-115.

Tsuchiya, Y., Nakajima, M., Itoh, S., Iwanari, M., & Yokoi, T. (2003). Expression of aryl hydrocarbon receptor repressor in normal human tissues and inducibility by polycyclic aromatic hydrocarbons in human tumor-derived cell lines. *Toxicological Sciences, 72*(2), 253-259.

Unit on Biological Hazards and Contaminants. (2018). *Information Session on the EFSA Opinion on PCDD/Fs and DL-PCBs in food and feed*. Paper presented at the Information Session on the EFSA Opinion on PCDD/Fs and DL-PCBs in food and feed, Parma, Italy https://www.efsa.europa.eu/sites/default/files/event/181113-report.pdf

Van den Berg, M., Birnbaum, L. S., Denison, M., De Vito, M., Farland, W., Feeley, M., . . . Peterson, R. E. (2006). The 2005 World Health Organization Reevaluation of Human and Mammalian Toxic Equivalency Factors for Dioxins and Dioxin-Like Compounds. *Toxicological Sciences, 93*(2), 223-241. doi:10.1093/toxsci/kfl055

Van den Berg, M., De Jongh, J., Poiger, H., & Olson, J. R. (1994). The toxicokinetics and metabolism of polychlorinated dibenzo-p-dioxins (PCDDs) and dibenzofurans (PCDFs) and their relevance for toxicity. *Critical reviews in toxicology, 24*(1), 1-74.

Vandesompele, J., De Preter, K., Pattyn, F., Poppe, B., Van Roy, N., De Paepe, A., & Speleman, F. (2002). Accurate normalization of real-time quantitative RT-PCR data by geometric averaging of multiple internal control genes. *Genome biology, 3*(7), 1-12.

VKM, H. K., Heidi Amlund, Jonny Beyer, Barbara Bukhvalova, , Dagrun Engeset, I. T. L. L., Espen Mariussen, Gro Haarklou , Mathisen, A. L. B., Sara Bremer, Ingunn Anita Samdal, Cathrine Thomsen,, & Eriksen, G. S. (2022). Risk assessment of dioxins, furans and dioxin-like PCBs in food in Norway. *Scientific Opinion of the Panel on Contaminants of the Norwegian Scientific Committee for Food and Environment., 2022:16*.

Volz, D. C., Bencic, D. C., Hinton, D. E., Law, J. M., & Kullman, S. W. (2005). 2, 3, 7, 8-Tetrachlorodibenzo-p-dioxin (TCDD) induces organ-specific differential gene expression in male Japanese medaka (Oryzias latipes). *Toxicological Sciences, 85*(1), 572-584.

Walker, N. J., Portier, C. J., Lax, S. F., Crofts, F. G., Li, Y., Lucier, G. W., & Sutter, T. R. (1999). Characterization of the dose–response of CYP1B1, CYP1A1, and CYP1A2 in the liver of female Sprague–Dawley rats following chronic exposure to 2, 3, 7, 8-tetrachlorodibenzo-p-dioxin. *Toxicology and Applied Pharmacology, 154*(3), 279-286.

Welsh, J. A., Jenkins, L. M., Kepley, J., Lyons, G. C., Moore, D. M., Traynor, T., . . . Jones, J. C. (2020). High sensitivity protein gel electrophoresis label compatible with mass-spectrometry. *Biosensors, 10*(11), 160.

Whitlock, J. P., Chichester, C. H., Bedgood, R. M., Okino, S. T., Ko, H. P., Ma, Q., . . . Clarkekatzenberg, R. (1997). Induction of drug-metabolizing enzymes by dioxin. *Drug metabolism reviews, 29*(4), 1107-1127.

Wiegel, J., & Wu, Q. (2000). Microbial reductive dehalogenation of polychlorinated biphenyls. *FEMS microbiology ecology, 32*(1), 1-15.

Wiest, E. F., Walsh-Wilcox, M. T., Rothe, M., Schunck, W.-H., & Walker, M. K. (2016). Dietary omega-3 polyunsaturated fatty acids prevent vascular dysfunction and attenuate cytochrome P4501A1 expression by 2, 3, 7, 8-tetrachlorodibenzo-p-dioxin. *Toxicological Sciences, 154*(1), 43-54.

Williams, S. R., Son, D.-S., & Terranova, P. F. (2004). Protein kinase C δ is activated in mouse ovarian surface epithelial cancer cells by 2, 3, 7, 8-tetrachlorodibenzo-p-dioxin (TCDD). *Toxicology, 195*(1), 1-17.

Wilson, K., & Walker, J. (2010). *Principles and techniques of biochemistry and molecular biology*: Cambridge university press.

Yamamoto, J., Ihara, K., Nakayama, H., Hikino, S., Satoh, K., Kubo, N., . . . Hara, T. (2004). Characteristic expression of aryl hydrocarbon receptor repressor gene in human tissues: organ-specific distribution and variable induction patterns in mononuclear cells. *Life sciences, 74*(8), 1039-1049.

Yang, J., Solaimani, P., Dong, H., Hammock, B., & Hankinson, O. (2013). Treatment of mice with 2, 3, 7, 8-Tetrachlorodibenzo-p-dioxin markedly increases the levels of a number of cytochrome P450 metabolites of omega-3 polyunsaturated fatty acids in the liver and lung. *The Journal of toxicological sciences, 38*(6), 833-836.

Zacharova, L. Y., Gulyaeva, L. F., Lyakhovich, V. V., Mikhailova, O. N., Timofeeva, O. A., Filipenko, M. L., & Kaledin, V. I. (2003). Cytochrome P4501A1 and 1A2 gene expression in the liver of 3-methylcholanthrene-and o-aminoazotoluene-treated mice: a comparison between PAH-responsive and PAH-nonresponsive strains. *Toxicological Sciences, 73*(1), 108-113.

Zhang, Z.-Y., Pelletier, R. D., Wong, Y. N., Sugawara, M., Zhao, N., & Littlefield, B. A. (2006). Preferential inducibility of CYP1A1 and CYP1A2 by TCDD: Differential regulation in primary human hepatocytes versus transformed human cells. *Biochemical and Biophysical Research Communications, 341*(2), 399-407. doi:https://doi.org/10.1016/j.bbrc.2005.12.203